

RESEARCH

Open Access



# The songbird connectome (OSCINE-NET.ORG): wstructure–function organization beyond the canonical vocal control network

Andrew Savoy<sup>1\*†</sup>, Katherine L. Anderson<sup>2,3\*†</sup> and Joseph V. Gogola<sup>4\*</sup>

## Abstract

**Background** Understanding the neural basis of behavior requires insight into how different brain systems coordinate with each other. Existing connectomes for various species have highlighted brain systems essential to various aspects of behavior, yet their application to complex learned behaviors remains limited. Research on vocal learning in songbirds has extensively focused on the vocal control network, though recent work implicates a variety of circuits in contributing to important aspects of vocal behavior. Thus, a more comprehensive understanding of brain-wide connectivity is essential to further assess the totality of circuitry underlying this complex learned behavior.

**Results** We present the **O**scine **S**tructural **C**onnectome for **I**vestigating **N**eural **N**etwork **O**rganizati**O**n (OSCINE-NET.ORG), the first interactive mesoscale connectome for any vocal learner. This comprehensive digital map includes all known connectivity data, covering major brain superstructures and functional networks. Our analysis reveals that the songbird brain exhibits small-world properties, with highly connected communities functionally designated as motor, visual, associative, vocal, social, and auditory. Moreover, there is a small set of significant connections across these communities, including from social and auditory sub-communities to vocal sub-communities, which highlight ethologically relevant facets of vocal learning and production. Notably, the vocal community contains the majority of the canonical vocal control network, as well as a variety of other nodes that are highly interconnected with it, meriting further evaluation for their inclusion in this network. A subset of nodes forms a "rich broker club," highly connected across the brain and forming a small circuit amongst themselves, indicating they may play a key role in information transfer broadly. Collectively, their bidirectional connectivity with multiple communities indicates they may act as liaisons across multiple functional circuits for a variety of complex behaviors.

**Conclusions** OSCINE-NET.ORG offers unprecedented access to detailed songbird connectivity data, promoting insight into the neural circuits underlying complex behaviors. This data emphasizes the importance of brain-wide integration in vocal learning, facilitating a potential reevaluation of the canonical vocal control network. Furthermore, we computationally identify a small, previously unidentified circuit—one which may play an impactful role in brain-wide coordination of multiple complex behaviors.

**Keywords** Oscine, Songbird, Vocal learning, Connectome, Graph theory, Network analysis

<sup>†</sup>Andrew Savoy and Katherine L. Anderson are co-first authors.

\*Correspondence:

Andrew Savoy  
savoy@uchicago.edu  
Katherine L. Anderson  
kanderson3@ccny.cuny.edu  
Joseph V. Gogola  
gogola@uchicago.edu

Full list of author information is available at the end of the article



© The Author(s) 2024. **Open Access** This article is licensed under a Creative Commons Attribution-NonCommercial-NoDerivatives 4.0 International License, which permits any non-commercial use, sharing, distribution and reproduction in any medium or format, as long as you give appropriate credit to the original author(s) and the source, provide a link to the Creative Commons licence, and indicate if you modified the licensed material. You do not have permission under this licence to share adapted material derived from this article or parts of it. The images or other third party material in this article are included in the article's Creative Commons licence, unless indicated otherwise in a credit line to the material. If material is not included in the article's Creative Commons licence and your intended use is not permitted by statutory regulation or exceeds the permitted use, you will need to obtain permission directly from the copyright holder. To view a copy of this licence, visit <http://creativecommons.org/licenses/by-nc-nd/4.0/>.

## Background

Learned behavior is complex, involving interactions between multiple brain systems. Understanding how these circuits coordinate with one another is necessary for understanding the neural basis of behavior. For instance, barn owls integrate auditory and visual cues to create a precise spatial map of the environment, a developmental learning phenomenon that requires anatomical reorganization and is essential to hunting behavior [1–3]. Pair bonding in prairie voles requires social, limbic, and cortical circuits, and is partially mediated by hormonal systems [4, 5]. In rhesus monkeys, a variety of cortical and subcortical circuits are involved in reward-based decision-making tasks, integrating sensory, reward, and memory mechanisms to guide learning [6, 7]. All of these behaviors rely on the functional integration of multiple brain networks to direct the acquisition of adaptive motor outputs. Therefore, to understand the neural control of learning and complex behaviors, it is necessary to understand the anatomical connectivity of brain-wide circuitry.

Constructing wiring diagrams and connectomes has provided valuable insight into brain-wide connectivity supporting behavior. The fruit fly connectome, FlyWire, has revealed corollary discharge circuits essential to flying, which might be common across insects [8–12]. Similarly, the Marmoset Brain Connectivity Atlas has been used to describe direct, non-reciprocal projections from auditory areas to the visual cortex in two primate species, indicating that early-stage audiovisual integration is a common trait in primate sensory processing [13]. Utilization of the Allen Mouse Brain Connectivity Atlas has suggested that functional circuits might be further parcellated by their structural inputs, allowing insight into how segregation and integration within and across circuits might be essential to drive behaviors [14, 15]. However, while these tools have enhanced our understanding of basic brain structures underlying important functional computations, their usefulness for interrogating complex learned behaviors is still in its infancy. This is due, in part, to circuit-level investigations often utilizing model systems where robust, complex behaviors have yet to be extensively characterized. To fully realize the potential of connectomics in elucidating the neural basis of behavior, we should utilize systems for which complex behaviors have been well-characterized, serving as a strong foundation for further study.

Vocal learning, a complex behavior that is common among several taxa, has been extensively characterized on a behavioral level. Among experimental models, the songbirds are the most thoroughly studied for the neural underpinnings of vocal learning. Behavioral studies have extensively documented vocal learning across closely

related species, and most neurobiological research has focused on the “vocal control network”: HVC (proper name), Area X (proper name), the dorsolateral nucleus of the medial thalamus (DLM), the lateral magnocellular nucleus of the anterior nidopallium (LMAN), the robust nucleus of the arcopallium (RA), the hypoglossal nucleus of the twelfth cranial nerve, tracheosyringeal portion (nXII[ts]), and the syrinx (the songbird vocal muscles). This network is common to all songbird species, contains regions and circuits functionally analogous to other vocal learners such as humans, and directly underlies vocal learning and production [16–18]. Indeed, much of the work in defining circuits anatomically has been directed at nodes in this network. This focused approach, while highly informative, has made it more difficult in assessing other brain systems more broadly. Yet, it may serve as the basis for a more comprehensive understanding of how distributed neural circuits might collaborate to support and modulate this complex behavior, and in how we might consider the vocal control network from a brain-wide perspective.

Indeed, recent research has highlighted the role of non-vocal brain circuits in influencing the perception and production of song. The physical environment impacts the molecular mechanisms of song perception, for example changing the context of a familiar song by altering the location of its playback or pairing it with synchronized light flashes reinitiates the genomic response associated with memory formation, indicating that associative learning circuits may be integral to vocal learning [19–22]. Similarly, the social environment biases both vocal learning and production, implicating social behavior circuits in the execution of these behaviors [23–27]. Dopaminergic circuits also play a crucial role in helping match motor output to vocal intent in song production, and while integrating social feedback about song quality [27, 28]. Finally, key connections between auditory and vocal-motor regions change toward the end of the critical period for vocal learning [29], suggesting age-dependent changes in how sensory information guides vocal behavior. Emphasizing the significant role of non-canonical vocal regions in various aspects of vocal learning and production, these findings necessitate a reevaluation of how information is received and processed by the vocal control network. This calls for a holistic understanding of brain-wide connectivity, particularly in the context of vocal learning and production.

Here, we present the **Oscine Structural Connectome for Investigating NEural NETwork ORGANIZATION** (OSCINE-NET.ORG), a comprehensive interactive digital map of anatomical connectivity among oscines. A synthesis of all known songbird neuroanatomical connectivity, this mesoscale connectome is a tool for exploring global

anatomic network structure and specialized circuitry for complex behaviors, particularly in the context of vocal learning and production. Graph theoretical analyses show the songbird brain is a small-world network, with groups of nodes forming highly connected communities. While these communities are well-connected within themselves by definition, there is differential connectivity across them, including amongst what we have defined as the associative, vocal, social, and auditory communities. We further identify several nodes that form a “rich broker club” of interconnected nodes with exceptionally high connectivity to the rest of the brain. Importantly, this club does not form its own community; its nodes are spread across multiple communities, and may act as crucial information relays for the entire network. These results demonstrate the importance of brain-wide circuitry pertaining to complex behaviors like vocal learning and production. They are meant to encourage expansive thinking about what brain regions might be considered a part of functional circuits, like the vocal control network. This work also serves as a reminder that vocal learning circuitry evolved in the context of other fundamentally important brain circuitry, reflecting the integrated nature of brain evolution and function.

## Methods

### Creation of the database and interactive website

The workflow used to generate the dataset is outlined in Fig. 1. We first collected literature that discussed connectivity data in any songbird brain, making no exclusion based on age, sex, or species. We did this in three ways. First, we utilized publically available citation databases Scopus, PubMed, and Google Scholar, using broad key search terms (e.g., “oscine”, “songbird”, “tracer”, “connection”, “circuit”, etc., and their combinations) to compile the available literature. Second, we used similar search terms in search engines such as Google Images to find published cartoons and diagrams of songbird brain circuits, and if their citations were missing from our literature list, they were added. Third, we did a more targeted search on individual author pages in Scopus, PubMed, and Google Scholar for well-known avian neuroanatomists, again adding in any missing literature to our list. Finally, using the revised avian nomenclature [30], we did an additional targeted search for regions that have had multiple common or accepted names throughout the years, using current and previous versions of acronyms, full common names, and full Latin names as additional search terms, again adding any missing literature to our list.

We included studies that describe anatomical connections (i.e., excluding solely functional data, such as functional magnetic resonance imaging) in all pallial and

subpallial superstructures of the songbird brain, as well as the periphery. We excluded data at the node level for multiple reasons:

*Migratory-specific nodes, as they are present in only a subset of all songbirds.*

*Peripheral ganglia, as they primarily shuttle sensory and motor signals between the periphery and the brain. Instead, connections that flow through ganglia were preserved as direct connections between the central and peripheral structure.*

*Vague or undefined nodes, such as those with unclear boundaries or only descriptions of approximate positions within a superstructure. This criterion was also applied to nodes named in non-songbird species when their equivalence to songbird nodes was unclear.*

*Unadopted subdivisions of nodes—subdivisions that have been proposed in the literature but have yet to be adopted by subsequent studies—were not subdivided. Adopted subdivisions were condensed when separation would have forced removal of a substantial amount of data under the Vague category, as earlier publications did not recognize these potential subdivisions.*

Using the collected data, we defined a list of nodes (brain regions or peripheral structures) and their superstructure (e.g., brainstem, nidopallium, etc.), using the revised avian nomenclature as an initial guide [30]. We compiled anatomical connectivity data for these nodes, making no distinction between nodes in the left or right hemisphere. We excluded data at the connection level for multiple reasons:

*Variable data, due to a lack of confidence in the biological status of these connections, including cases in which connections were found in only a subset of individuals, or when the authors expressed uncertainty about their data.*

*Internal connectivity, or the connections within a brain region (node), are not informative to mesoscale connectivity. This criterion was also applied to contralateral connections of the same node.*

*Theorized connections, or those assumed to be present in songbirds due to evolutionary conservation across taxa but for which no anatomical data exists. Nodes with no reported anatomical connections, or nodes defined on cytoarchitectural or neurochemical grounds, but with no reported anatomical connectivity.*

All data that passed the node-level and connection-level bottlenecks were compiled before further visualization and analysis, and are appended as Additional

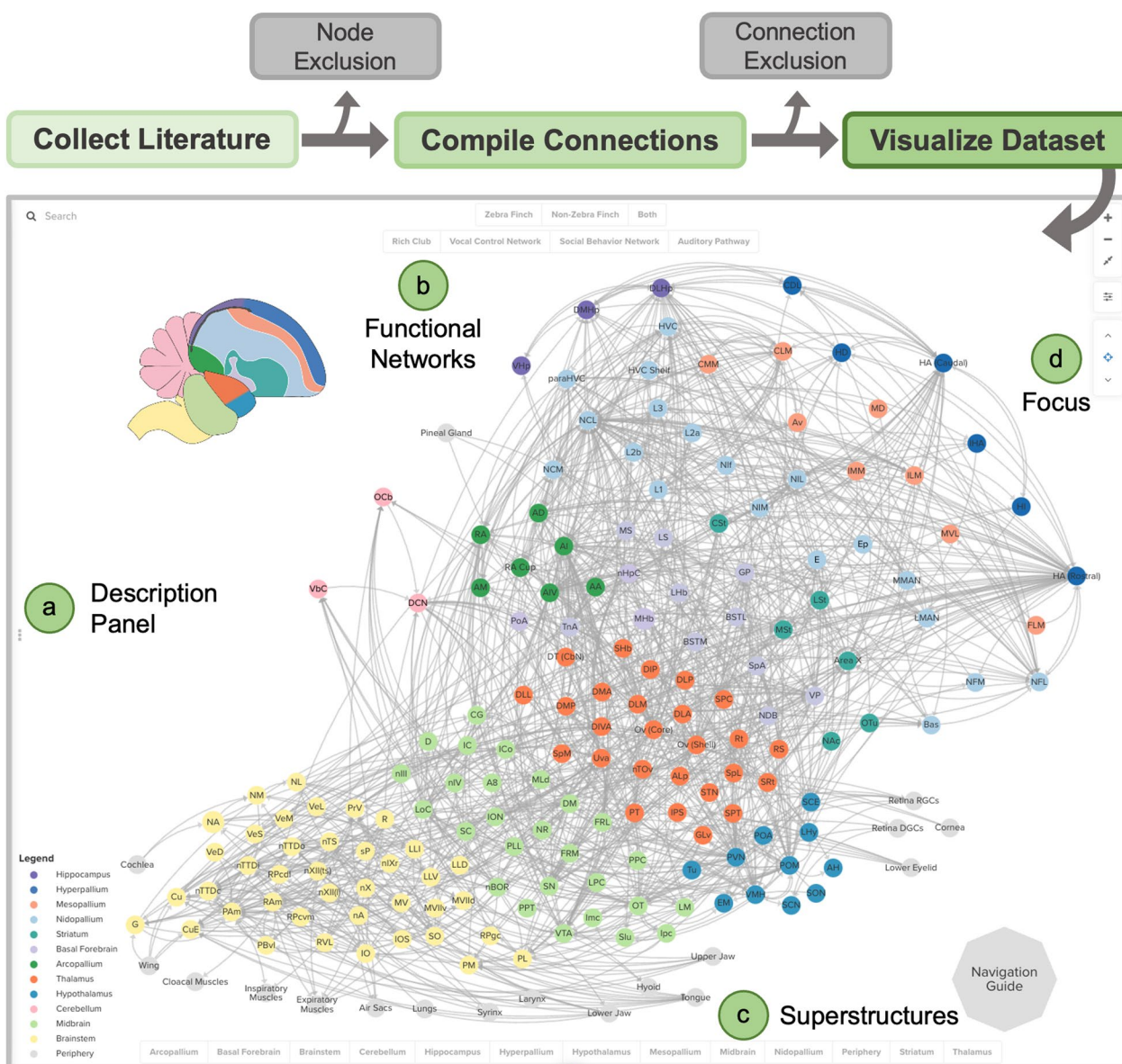


**Fig. 1** Curation and Visualization of the Oscine Structural Connectome for Investigating **NE**ural **NE**twork **OR**ganization (OSCINE-NET.ORG). Nodes and connections were trimmed from the present dataset at two exclusion bottlenecks (described in Methods). **a** The homepage of the anatomical connections map contains a general description panel that introduces the map and provides a link to a continuously updated Google Sheet of all connections, as well as **b** buttons to focus on nodes from select functional networks or **c** brain superstructures. **d** The connections to and from an individual node can be highlighted and navigated by level of connection using the focus buttons. Defined brain regions and widely used subdivisions are displayed as individual nodes (circles), color-coded by superstructure. Nodes are placed approximately within each superstructure, condensed onto a single sagittal plane. Anatomical connections are represented by gray arrows, which can be clicked on to view citation information in the side panel

file 1. Data was in no way scaled based on the number of times it appeared in our compiled list; that is, a connection that has been independently verified across 10 separate studies was not weighted any differently than a connection that has only been reported once.

The database was visualized using a freely available online tool [31], and an interactive version of the map is accessible at OSCINE-NET.ORG. The brain is represented as a single compressed sagittal plane, with nodes placed at their approximate location within the brain. Nodes are color-coded based on their superstructure membership, and

connections between nodes are indicated with a directed arrow. Description panels for each connection include reference citations and descriptive information for each study (e.g., species, sex, age, etc.), and description panels for each node include the unabbreviated node name. Further information on tool navigation, use of this tool, and a link to the underlying database can be found in the website's navigation guide.

### Global and node-level analyses

To analyze this database, we first constructed an adjacency matrix corresponding to the unweighted directed graph. Each entry was assigned a value of 1 where we find evidence of connectivity between pairs of nodes in our dataset, or 0 where we find no evidence of connectivity. This matrix, containing 187 nodes and 1107 connections, was used for further global- and node-level analyses. Analyses were computed using the NetworkX package in Python unless stated otherwise [32].

### Small-world analysis

To ask whether most nodes can be reached through a relatively short number of connections, we assessed the small-world properties of this network. We first calculated average path length (the distance between two nodes;  $\lambda$ ) and clustering coefficient (how likely a node's neighbors are to be connected to each other, forming tightly knit groups;  $\gamma$ ) for our network. We then constructed random graphs using two methods. The first method used the Erdős–Rényi model [33] to create random directed graphs with the same number of nodes and connections as our network. The second method employed the directed configuration model [34] to preserve our original network's in-degree and out-degree sequences (where "degree" refers to the number of incoming and outgoing connections for each node, respectively). We calculated average path length and clustering coefficient from these two methods, averaged over 1000 iterations each, for further analyses.

We used these random models to create two indices. The small-world index ( $\sigma$ ) is defined as the ratio of the average clustering coefficient of the original and the Erdős–Rényi model random network, divided by the ratio of the average path length of the original and the random network. The small world index for the degree-preserving directed configuration model random network ( $\sigma_{io}$ ) is similarly defined:

$$\sigma = \frac{\gamma/\gamma_r}{\lambda/\lambda_r} \quad \sigma_{io} = \frac{\gamma/\gamma_{rio}}{\lambda/\lambda_{rio}}$$

where  $\gamma$  is the clustering coefficient of the network, and  $\lambda$  is the average path length;  $\gamma_r$  and  $\lambda_r$  are the clustering coefficient and average path length, respectively, of a random network; and  $\gamma_{rio}$  and  $\lambda_{rio}$  are the clustering

coefficient and average path length of a degree-preserving random network. Z-scores were used to measure the significance of the differences.

### Assortativity

To assess assortativity—the tendency for nodes to connect to other nodes of the same degree—we calculated the degree assortativity coefficient as the Pearson correlation between the degrees of connected nodes [35]:

$$r = \frac{\sum_{jk} jk(e_{jk} - q_j q_k)}{\sigma_q^2}$$

where  $e_{jk}$  is the joint probability distribution of the degrees of two, randomly chosen, connected nodes,  $q_j$  and  $q_k$  are the degree distributions, and  $\sigma_q$  is the standard deviation of the degree distribution.

### Community detection and analysis

To identify densely connected groups of nodes within the network, we used the RBConfigurationVertexPartition version of the Leiden algorithm for community detection using the *leidenalg* Python package [36]. This algorithm is suitable for unweighted directed graphs, such as ours, and guarantees connected communities. In addition, it maximizes a quality function to determine optimal modularity, a measure of the strength of division of a network into subgraphs—in other words, it determines how well nodes are grouped into communities within a network.

We ran the Leiden algorithm over 1000 iterations, each with a different random seed. We calculated the Adjusted Mutual Information [37] score between every pair of communities across all random iterations. The seed with the highest average Adjusted Mutual Information score represented the most stable community structure. Using the most stable seed, we re-ran the Leiden algorithm to obtain the representative community delineations. To validate the representative community delineations, we plotted the distribution of community counts across all resolutions (a parameter that affects size of communities) in increments of 0.05 from 0.5 to 1.5 over 100 iterations to find the resolution value that tends to produce the mean number of communities detected, then re-ran the most stable seed at that resolution.

The modularity optimized by the RBConfigurationVertexPartition version of the Leiden algorithm is given by:

$$Q = \sum_{ij} \left( A_{ij} - \gamma \frac{k_i k_j}{2m} \right) \delta(c_i, c_j)$$

where  $A_{ij}$  is the adjacency matrix,  $k_i$  and  $k_j$  are the degrees of nodes  $i$  and  $j$ ,  $m$  is the total number of connections,  $\gamma$  is

the resolution parameter, and  $\delta(c_i, c_j)$  is equal to 1 if nodes  $i$  and  $j$  are in the same community, and 0 otherwise.

### Sub-community detection and analysis

We detected sub-communities within each community delineation by applying the RBConfigurationVertexPartition version of the Leiden algorithm recursively, with a sub-resolution parameter of 0.75, constructing sub-communities for each community. We generated a null model to assess sub-community connectivity with other sub-communities, excluding self-self connections. We normalized counts to the product of the size of each sub-community pair, shuffled over 1000 iterations while maintaining the total number of connections across the subset matrix, and determined significance with permutation tests in R (v3.6.2).

### Centrality metrics

Centrality metrics, such as degree and betweenness centrality, are fundamental methods for quantifying the importance or influence of individual nodes in a network [38]. Degree is the sum of total inputs to a single node (in-degree) and total outputs of the same node (out-degree); more simply, it is the total number of connections a node makes. We quantified degree centrality as each node's degree divided by the maximum possible degree for this network:

$$C_D(v) = \frac{\text{deg}(v)}{N - 1}$$

where  $\text{deg}(v)$  is the total degree of node  $v$ , and  $N$  is the total number of nodes.

Betweenness centrality is the frequency at which a node lies on the shortest path between two nodes, or its capacity to serve as a "bridge" between two nodes:

$$C_B(v) = \sum_{s,t \in V} \frac{\sigma(s, t|v)}{\sigma(s, t)}$$

where  $\sigma(s, t)$  is the total number of shortest paths from node  $s$  to node  $t$ ,  $\sigma(s, t|v)$  is the number of those paths passing through node  $v$ , and  $V$  is the set of nodes in the graph.

Principal component analysis was performed on the degree centrality, betweenness centrality, closeness centrality, and clustering coefficient. Scree plots of eigenvalues were generated and loadings extracted to determine percent variance explained. Elbow plots were generated using within-cluster sum of squares, and k-means clustering was applied for visual representation of clusters. Scatterplots were generated for the two centrality metrics that explained the greatest percent variance, by plotting degree centrality against betweenness centrality. As

a more intuitive alternative, we have presented a plot of degree against betweenness centrality, which is identical.

### Rich club coefficient analysis

We used the rich club coefficient analysis to discern whether nodes with high centrality tend to be more densely interconnected among themselves than expected by chance [39]. The rich club coefficient for a directed graph is given by:

$$\phi(k) = \frac{E_{>k}}{N_{>k}(N_{>k} - 1)}$$

where  $\phi(k)$  is the rich club coefficient for nodes with degree greater than  $k$ ,  $E_{>k}$  is the number of connections among the nodes with degree greater than  $k$ , and  $N_{>k}$  is the number of nodes with degree greater than  $k$ .

First, each degree served as an arbitrary degree threshold ( $k$ ), starting from 1 (the minimum degree for a node in the network) to the maximum degree for a node in the network (past which the degree size would be unexpected in a random network). Then, the rich club coefficient was calculated by isolating nodes with degree past that arbitrary threshold, and normalized to the total number of possible connections between those nodes. For each degree threshold, we created 1000 random graphs using a directed configuration model to compute the mean and standard deviation of the rich club coefficients for the random graphs. A given degree threshold  $k$  justifies membership in the "rich club" if the observed rich club coefficient is more than one standard deviation above the mean of the random graphs. Nodes that are part of the rich club are, therefore, both nodes with many connections ("rich"), and tend to form a highly interconnected group within themselves ("club").

## Results

### The first publicly available mesoscale connectome for any vocal learner

The **O**scine **S**tructural **C**onnectome for **I**nvestigating **N**eural **N**ETwork **O**Rganization (OSCINE-NET.ORG) is a public access database of anatomical connectivity across the songbird brain. OSCINE-NET.ORG is an interactive connectome of the songbird brain, and covers a range of brain superstructures, functional networks, and peripheral systems (Fig. 1). The database summarizes the entire connectivity dataset analyzed here, consisting of 187 nodes and 1107 connections (as of July 26, 2024). The database, which will be continually updated as new data are published, is accessible via a maintained spreadsheet that is linked in the Navigation Guide and homepage description panel (Fig. 1a). The data used to run the graph theoretical analyses presented in this paper is

available as a supplement (Additional File 1), as is a full list of works cited in the database (Additional file 2).

The database includes connectivity data from 14 oscine songbird species (Table 1). Connections in zebra finches represent 78.7% of the data (1286 out of 1634 entries), with contributions from other species ranging from 0.12% to 4.35% of entries. The number of

supporting citation entries for each connection ranges from 1 to 16, with 73.5% (815 out of 1107) of connections supported by a single study. For connections supported by a single study, 77.8% (634 out of 815) of those studies were in zebra finches. Similarly, the compiled dataset is primarily from studies in adult males; 10.5% (117/1107) of connections in this database are from females.

When considering nodes that have been the subject of circuit mapping studies (Table 2), there has been a biased interest in the vocal control network. HVC, Area X, and RA are the top three most-reported injection sites with, respectively, 19, 18, and 17 independent studies focused on these nodes. This undoubtedly biases our database and subsequent analyses, where for instance many nodes in the vocal control network might be considered relatively completely described in terms of their brain-wide connections. In contrast, 41.2% (77/187) of included nodes in our database have never been the focus of a circuit mapping study. This leaves many gaps in our knowledge and database, where reported connectivity of these nodes is solely reliant on studies focused on other nodes and undoubtedly does not describe the totality of their brain-wide connections. The skew of these data represents the objective breadth of published anatomical connectivity studies in songbirds, and not a subjective choice of focus in our data collection or reporting.

**Table 1** Species representation of entries in the compiled database

Species	Number of entries
Bengalese Finch ( <i>Lonchura striata domestica</i> )	47 (2.88%)
Black-Capped Chickadee ( <i>Poecile atricapillus</i> )	26 (1.59%)
Canary ( <i>Serinus canaria</i> )	71 (4.35%)
Carrion Crow ( <i>Corvus corone</i> )	27 (1.65%)
Eurasian Blackcap ( <i>Sylvia atricapilla</i> )	12 (0.73%)
European Starling ( <i>Sturnus vulgaris</i> )	59 (3.61%)
Garden Warbler ( <i>Sylvia borin</i> )	16 (0.98%)
Greenfinch ( <i>Chloris chloris</i> )	24 (1.47%)
Hawfinch ( <i>Coccothraustes coccothraustes</i> )	2 (0.12%)
House Finch ( <i>Haemorhous mexicanus</i> )	39 (2.39%)
House Sparrow ( <i>Passer domesticus</i> )	6 (0.37%)
Jackdaw ( <i>Corvus monedula</i> )	5 (0.31%)
Java Sparrow ( <i>Padda oryzivora</i> )	2 (0.12%)
Zebra Finch ( <i>Taeniopygia guttata</i> )	1286 (78.7%)
Total	1634

Number of entries per species, and the percent of entries in the database they represent

**Table 2** Distribution of studies focused on specific nodes

Number of studies	Node
19	HVC
18	Area X
17	RA
12	LMAN, NCL
9	Uva
7	DLHp, VP, VTA
6	AI, HA (Rostral), NCM
5	DLM, DMHp, MSt, Nif, NIL, RAm
4	AIV, Av, Cu, HA (Caudal), LLV, LM, MLd, NFL, OT, Retina RGCs, SN
3	Bas, CLM, CuE, DCN, DM, G, ICo, LLI, LoC, MMAN, NA, nBOR, NL, nXII(ts), OCb, PAm, PrV, RA Cup, RVL, VbC
2	CG, CSt, DIVA, DMP, DT (CbN), E, GP, HVC Shelf, L2b, LLD, LSt, NAC, NM, nTTDi, Ov (Core), Ov (Shell), PVN, Rt, SO, SpM, Upper Jaw, VHp
1	Air Sacs, Cloacal Muscles, CMM, Expiratory Muscles, GLv, Hyoid, ILM, Inspiratory Muscles, Ipc, L1, L2a, L3, Larynx, LHb, Lower Eyelid, Lower Jaw, Lungs, MV, MVIIId, MVL, NIM, NR, nTS, nTTDc, nTTDo, paraHVC, PBvl, Pineal Gland, PL, POM, RPcvm, SC, SC, STN, Syrinx, TnA, Tongue, VeS, VMH, Wing
0	A8, AA, AD, AH, ALp, AM, BSTL, BSTM, CDL, Cochlea, D, DIP, DLA, DLL, DLP, DMA, EM, Ep, FLM, FRL, FRM, HD, HI, IC, IHA, Imc, IMM, IO, ION, IOS, IPS, LHv, LPC, LS, MD, MHb, MS, MVIIv, nA, NDB, Neck, NFM, nHpC, nIII, nIV, nIXr, nTOv, nX, nXII(I), OTu, PLL, PM, POA, PoA, PPC, PPT, PT, R, Retina DGCs, RPcdl, RPgc, RS, SCN, SHb, Slu, SON, sP, SpA, SPC, SpL, SPT, SRt, SSp, Tu, VeD, VeL, VeM

We report the total number of citations in our dataset where each node was the focus of the study (e.g., tracer injection directly into that node to map its connectivity). Nodes are organized in alphabetical order within each row. Full names of node abbreviations can be found in the Abbreviations

### The songbird brain is a small-world network, organized into tightly-clustered communities

This network has a clustering coefficient of 0.25, significantly higher than that of random networks ( $\gamma_r=0.03$ ,  $z\text{-score}=109.32$ ,  $p<0.001$ ) and degree-preserving random networks ( $\gamma_{r10}=0.08$ ,  $z\text{-score}=26.08$ ,  $p<0.001$ ). The average path length ( $\lambda$ ) of 3.14 is significantly higher than the average path length for degree-preserving random networks ( $\lambda_{r10}=3.05$ ,  $z\text{-score}=3.11$ ,  $p=0.002$ ), but not for random networks ( $\lambda_r=3.13$ ,  $z\text{-score}=1.04$ ,  $p=0.29$ ). The small-world index ( $\sigma$ ) of 2.67 and the normalized small-world index ( $\sigma_{i0}$ ) of 2.94 confirm the network's small-world nature, emphasizing its efficient balance of local clustering and global integration. For the normalized small-world index ( $\sigma_{i0}$ ), these values are higher than corresponding significant indices for macaque cortex ( $\sigma_{i0}=1.7050$ ), cat cortex ( $\sigma_{i0}=1.3027$ ), and pigeon pallium ( $\sigma_{i0}=1.4004$ ) [40, 41]. While the Allen Institute mesoscale connectome of the mouse did not quantify this specific metric, they report similar small-world properties in their network [14]. Thus, similar to other vertebrate mesoscale connectomes, the songbird brain also has small-world properties.

The assortativity coefficient of the network is  $r=-0.13$ . Negative assortativity indicates disassortative mixing [35], or a bias in favor of connections between nodes dissimilar in degree. This is true for networks with a small number of highly connected hubs and a large number of low-degree nodes. Negative assortativity is common in biological networks [42, 43], including in a mesoscale connectome of the pigeon, a non-songbird [41].

To identify communities with shared connectivity patterns, we utilized the Leiden algorithm for modularity-based community detection. Our methods yield a consensus matrix of 6 communities, (Fig. 2), near the average of 6.33, detected over 1000 random iterations. Each community has two or three sub-communities. The full list of communities, sub-communities, and nodes is presented in Table 3, and nodes are organized in the same manner as in the matrix, listed by sub-community nested within their primary community. Nodes are organized within each sub-community by descending number of total connections. Full names of nodes are available in the Abbreviations.

By definition, communities are groups of nodes that are highly connected within themselves. Many of the nodes in each community have well-known functional roles, which strongly support the following designations: 1) motor, 2) visual, 3) associative, 4) vocal, 5) social, and 6) auditory. The motor community contains the majority of peripheral structures (13/18) and motor neuron pools (6/9) in the network. The visual

community contains peripheral, thalamic, and tectal-visual sensory regions, downstream brainstem and cerebellar processing centers, and the motor neurons that control eye movements [44–46]. The associative community contains the main associative learning regions of the songbird brain [47–49], as well as a diverse set of higher visual, somatosensory, and premotor regions [50, 51]. The vocal community contains the majority of nodes in the canonical vocal control network (5/7), as well as numerous nodes that have been implicated in vocal learning and production by others [52–54] (see Discussion). The social community contains the majority of nodes in the social behavior network (6/8), as well as many other septal, hippocampal, and viscerolimbic nodes with well-known roles in social behaviors [55–57]. The auditory community contains all of the classically defined auditory nodes, including basic auditory sensory [58–60] and higher-order perceptual nodes [61–63]. Thus, these community designations are well-founded, and a useful anchor in considering what connectivity across these communities might mean for complex behaviors. We don't claim these as definitive designations, nor that their individual nodes should now be categorically considered part of these circuits; we only mean to use these computationally-defined communities to encourage more expansive thinking about what nodes might be considered parts of different functional circuits, based on similar connectivity profiles.

Next, to ask how communities might communicate with each other, we visualized inter-community connectivity with a chord diagram (Fig. 3A), where chords between communities are weighted to the total number of connections in the pair. We find that a subset of sub-communities preferentially connect with each other (Fig. 3B). The vocal community tends to receive inputs from the auditory ( $p=0.008$ ) and social community ( $p=0.037$ ), and send outputs to both associative sub-communities (to sub-community 3a,  $p=0.045$ ; to sub-community 3b,  $p=0.017$ ). In addition to the vocal community inputs, the associative community tends to receive inputs from the auditory community ( $p=0.012$ ), and send outputs to the social community ( $p=0.043$ ) and the vocal community (from sub-community 3a,  $p=0.027$ ; from sub-community 3b,  $p=0.016$ ). All significant connections between sub-communities are condensed in Fig. 3C. Thus, while communities and sub-communities are defined by their high connectivity within themselves, there is a bias in how these communities connect with each other, informing how different functional circuits might share various streams of information that are essential to complex behaviors.

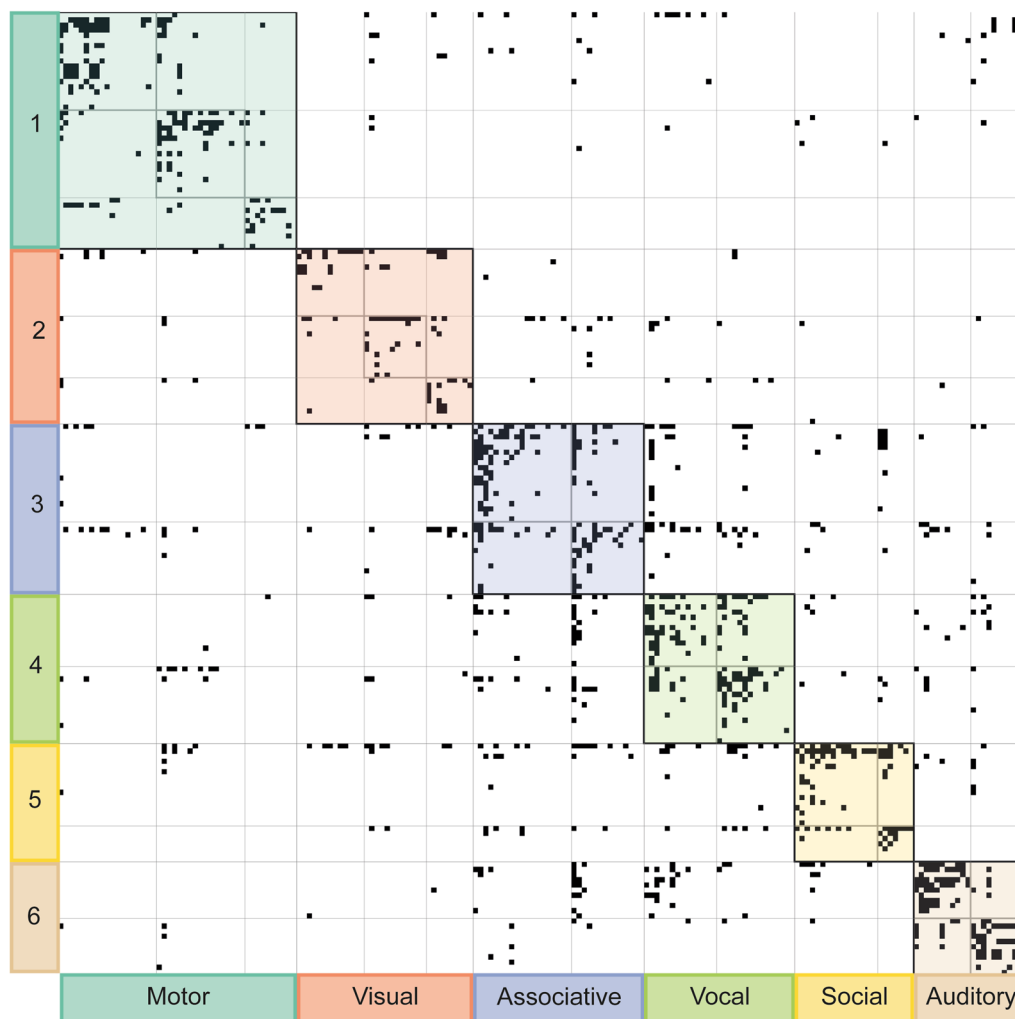


**Fig. 2** Community detection partitions nodes into six highly-interconnected communities. Communities (shaded groups along the diagonal) and their respective sub-communities (smallest squares along the diagonal) are shown. Each row depicts all connections a node sends, while its corresponding column depicts all the connections it receives. Within sub-communities, nodes are in descending order of degree. The nodes making up each community and sub-community are presented in Table 3, organized in the same manner

### Differential connectivity patterns of the vocal control nodes and the vocal sub-communities suggest differing roles in the network

We next asked how the individual nodes in a community might connect with other communities. We focused on the vocal control network, since it is mostly contained within the vocal community: HVC, RA, DLM, LMAN, and Area X fall into the vocal community, while nXII(ts) and the syrinx are in the motor community (Fig. 4A, B). While most of these nodes primarily receive inputs from and send outputs to their own communities, there are a few notable outliers. Excluding canonical vocal control network connectivity, Area X primarily receives input from the associative community, with 12/27 connections, compared to its inputs from the vocal community at 11/27

connections (Fig. 4A). Similarly, RA sends equal outputs to the motor and vocal communities, each receiving 6/14 connections (Fig. 4B). While the vocal control network mostly falls into the vocal community, there is separation of these nodes into the two vocal sub-communities: HVC, Area X, and LMAN are in vocal sub-community 4a, while RA and DLM are in vocal sub-community 4b (Fig. 4C).

These sub-communities have some notable similarities in their connections with the non-vocal communities (Fig. 4D). Aside from connections with the vocal community nodes, vocal sub-communities 4a and 4b each primarily receive inputs from and send outputs to the associative community. The next highest community interactions for vocal sub-community 4a is with

**Table 3** Communities and sub-communities designations.

Community	Sub-community	Nodes
1 Motor	1a	Uva, nTTDc, nTTDi, nTTDo, Cu, PrV, CuE, DIVA, IO, G, Lower Jaw, Upper Jaw, Lower Eyelid, RS, Wing, Syrinx, VeM, sP, Cornea
	1b	PAm, ICo, RAm, DM, nTS, RVL, R, nXII(ts), NR, Expiratory Muscles, PBvl, IOS, Air Sacs, VeD, Inspiratory Muscles, Lungs, Cloacal Muscles
	1c	MV, Tongue, RPcvm, MVlId, RPcdl, MVlIv, nXII(l), nIXr, Hyoid, nX
2 Visual	2a	nBOR, LM, PM, Retina RGCs, Retina DGCS, DLA, SCN, ION, IC, nIV, D, VeL, nIII
	2b	OT, CG, Rt, GLv, EM, lpc, lmc, SPT, RPgc, IPS, Slu, SON
	2c	DCN, PL, Ocb, VbC, SpM, PPC, LPC, ALp, SpA
3 Associative	3a	AI, NIL, HA (Caudal), NFL, HD, IMM, ILM, Bas, NIM, CDL, FRL, PT, DLL, HI, DIP, VeS, SPC, DLP, PLL
	3b	NCL, HA (Rostral), GP, E, LSt, SRt, SCE, FRM, MVL, SpL, NFM, AA, FLM, Ep
4 Vocal	4a	AIV, Area X, HVC, AD, DMP, CSt, paraHVC, LMAN, Nif, MMAN, SC, Av, DT (CbN), MD
	4b	RA, VP, LoC, VTA, SN, MSt, DLM, STN, LHb, NAc, DMA, PPT, nA, Larynx, A8
5 Social	5a	PVN, POM, TnA, VMH, AM, LHv, LS, BSTL, PoA, MHb, POA, BSTM, Pineal Gland, nHpC, AH, Tu
	5b	DLHp, DMHp, MS, VHp, NDB, SHb, OTu
6 Auditory	6a	Ov (Shell), CLM, NCM, L3, L1, nTOv, HVC Shelf, L2a, L2b, CMM, IHA
	6b	Ov (Core), LLV, MLd, RA Cup, SO, LLD, NA, NL, LLI, NM, Cochlea

Nodes are presented by their community and sub-community membership, organized in the same manner as Fig. 2, by descending order of degree within each sub-community. Full names of node abbreviations can be found in the Abbreviations

the auditory community. However, vocal sub-community 4b shows differential connectivity patterns after the two highest interacting communities. Vocal sub-community 4b receives its second greatest number of inputs from the social community, and sends its second most outputs to the motor community. These data highlight potential anatomical biases of each vocal sub-community for signal integration and communication.

#### A small set of nodes are highly connected with the rest of the network

We next investigated how individual nodes might organize based on connectivity features, irrespective of community. We calculated several metrics to assess this type of node-level organization. Nodes are described by their degree (total number of connections), in-degree (number of input connections), out-degree (number of output connections) and betweenness centrality (the extent to which a node lies on the shortest path between nodes, i.e. its capacity to serve as a bridge or “broker” between nodes). The top 5% of nodes for each metric are reported in Table 3, along with nodes in the canonical vocal control network. All metrics for all nodes are provided as supplement to this article (Additional file 3).

We find several nodes which are in the top 5% across multiple metrics: the caudolateral nidopallium (NCL), the rostral portion of the hyperpallium apicale (HA [Rostral]), the intermediate arcopallium (AI), the paraventricular nucleus of the hypothalamus (PVN), the medial preoptic nucleus of the hypothalamus (POM), the optic tectum (OT), and nucleus uvaeformis (Uva).

All these nodes are in the top 5% of degree. A subset of these nodes are also in the top 5% of in-degree (NCL, Uva), out-degree (PVN, POM, OT), or both (HA [Rostral], AI). Interestingly, the top 5% highest degree nodes are also often the top 5% for betweenness centrality, indicating they are among the most well-connected nodes in the network and have a high capacity to serve as brokers. Notably, none of the canonical vocal control network nodes falls into the top 5% for degree or out-degree. Two vocal control network nodes fall into the top 5% of in-degree (Area X and HVC), while one falls in the top 5% for betweenness centrality (RA).

#### The rich broker club: key hubs poised to direct information flow across the brain

Given that a common set of nodes frequently ranks in the top 5% across multiple node-level metrics, we sought to understand how these nodes relate to the rest of the network. To achieve this, we first applied principal component analysis to reduce the dimensionality of our data and highlight patterns. We then applied k-means clustering to the reduced-dimensionality data to clearly delineate these clusters (Fig. 5A). This shows that the seven nodes are separated from the rest of the network in high-dimensional space, suggesting they have properties that distinguish them from the others.

Next, we performed a rich club coefficient analysis to determine whether these nodes are highly interconnected. This analysis identifies nodes with a degree of 48 or higher as members of the rich club, meaning they both have high degree and are more densely interconnected

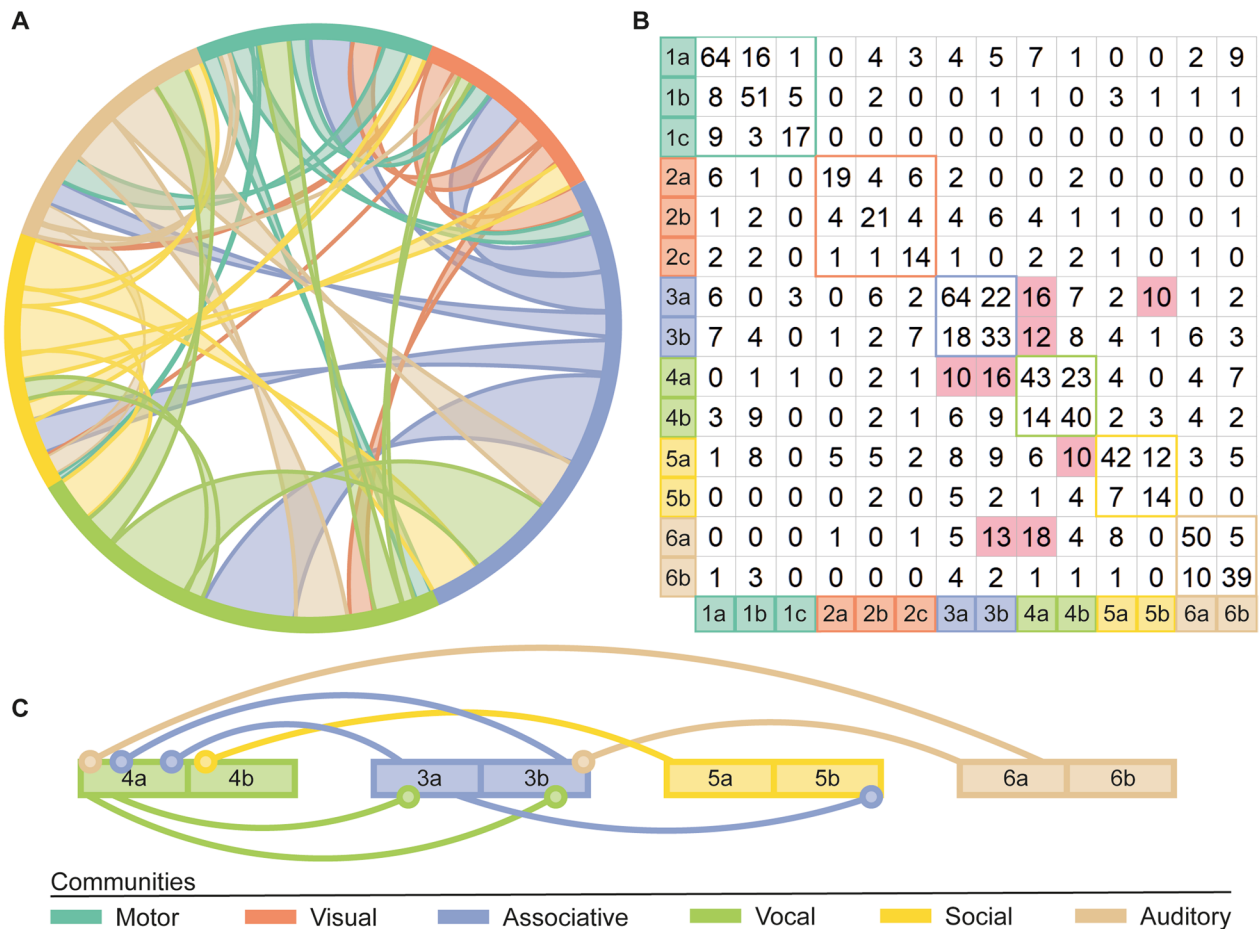


**Fig. 3** Cross-community analysis identifies connectivity structure at the level of sub-communities. **A** Community-to-community connections are represented by chords, weighted to the number of connections. Communities are color-coded in the same way as Fig. 2, and chords are color-coded by the sending community. **B** Raw number of sub-community to sub-community connections are shown at each intersection, organized so that each row depicts the number of connections a sub-community sends to each other sub-community, and its corresponding column depicts the connections it receives from each other sub-community. Sub-communities that demonstrate higher connection frequencies than chance are highlighted in pink ( $p < 0.05$ ). Sub-communities are defined in part by their high connectivity within themselves, so their significance is not highlighted here (see Fig. 2). **C** Representation of significant connection frequencies between sub-communities is shown in **B**. Color of connections indicate the origin sub-community of the connection

among themselves than expected by chance. These rich club members (and their degree) are NCL [65], HA (Rostral) [57], AI [52], and PVN [48] (Fig. 5B), which are four of the seven nodes of the cluster previously identified, reinforcing their significance. Considering that the rich club analysis is heavily influenced by node degree, and that the data in Table 4 shows these nodes also have high betweenness centrality, we suspected that these two dimensions (degree and betweenness centrality) would be sufficient to explain the clustering of these nodes. To confirm this, we plotted degree against betweenness centrality in a scatterplot (Fig. 5C). This plot demonstrates that the same set of seven nodes identified via dimensionality reduction and clustering analysis also separates

clearly from all other nodes (blue dots), thus the majority of the variance in the data can be explained by these two metrics.

To capture the multifaceted roles of these influential nodes, we introduce the concept of the “rich broker club” (Fig. 5D). This designation merges rich club nodes (highly interconnected and connected with the rest of the network) with broker nodes (high betweenness centrality), aiming to provide a more comprehensive understanding of their importance in the network. The rich broker club members are NCL, HA (Rostral), AI, PVN, POM, OT, and Uva. The rich broker club is well-connected with itself, and its members span six brain superstructures and four communities (Fig. 5D). Notably, each node in the

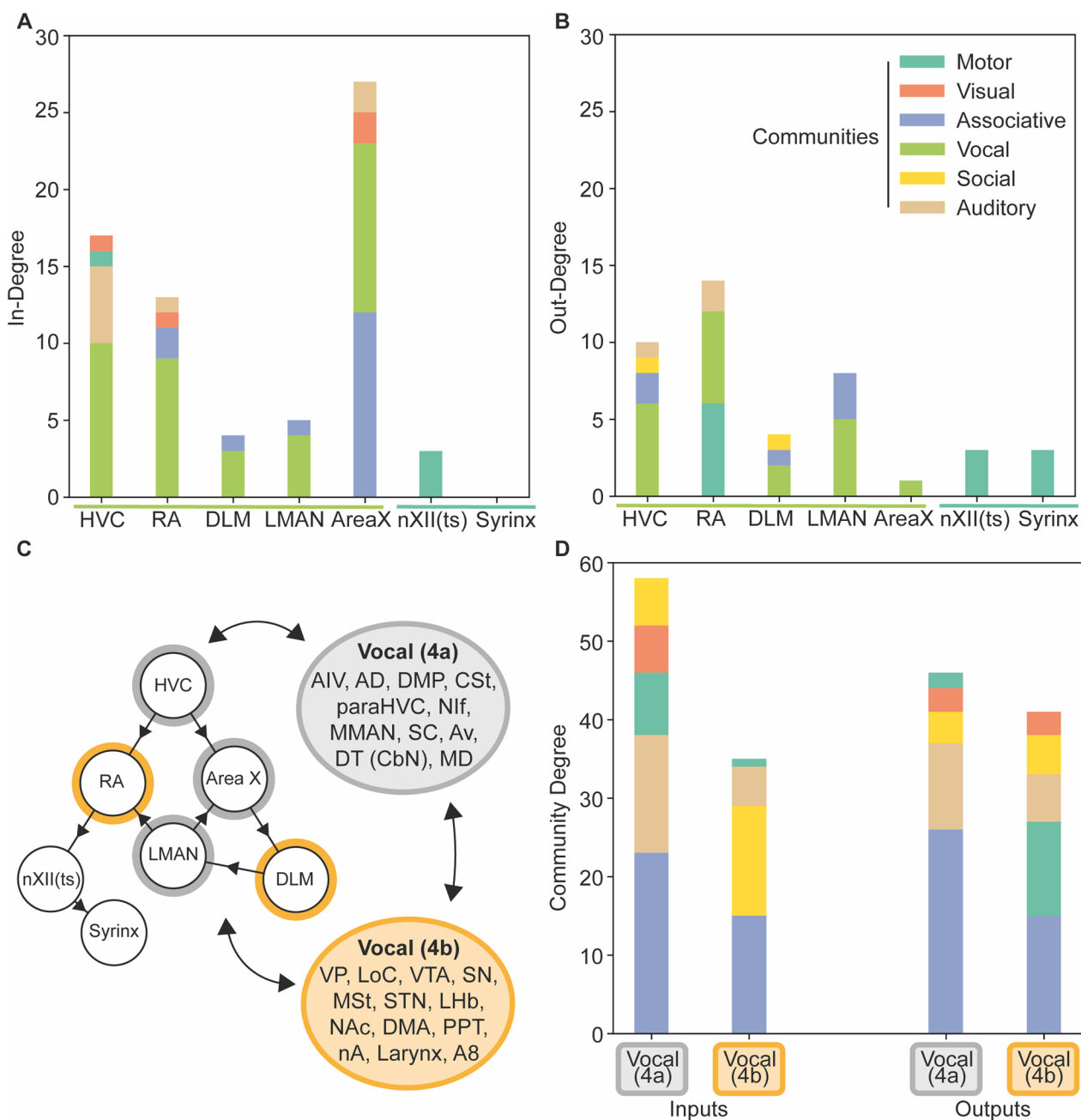


**Fig. 4** The vocal control network is split between vocal sub-communities, which have different community connectivity. In-degree (**A**) and out-degree (**B**) of each canonical vocal control network node to all communities, excluding canonical connections diagrammed in **C**. In- and out-degrees for each community are stacked such that the community with the highest number of connections to a node is lowest within the bar. **C** Canonical connections of the songbird vocal control network. The two vocal sub-communities, and their member nodes, are color-coded. Non-canonical vocal control network nodes are condensed into a single bubble per community. **D** In- and out-degree of all nodes in each vocal sub-community. Connections to and from the vocal community are excluded to highlight connections outside the vocal sub-communities. Bars are stacked in the same manner as **A** and **B**

rich broker club connects with most or all of our identified communities, as measured by in-degree (Fig. 5E) and out-degree (Fig. 5F). As a whole, the rich broker club accounts for 28.7% of connections in the network

(318/1107), and connects to 70.6% of nodes (132/187). Notably, nodes in the rich broker club have bidirectional connectivity with multiple communities, suggesting this club may serve a liaison role in connecting

various functional circuits (Fig. 6). Thus, the rich broker club is well-positioned to act as a set of key transmitters throughout the brain, linking multiple superstructures, communities, and functional circuits, and may be important for many complex behaviors.

## Discussion

OSCINE-NET.ORG is the first comprehensive, interactive, mesoscale wiring diagram of anatomical connectivity between brain areas and across every superstructure of the songbird brain—a major step toward a complete oscine connectome, and a valuable tool for investigating network organization. While there have long been useful tools available for songbird researchers pertaining to gross anatomy, morphology, and gene expression [64–68], there has been an noticeable lack of accessible and comprehensive resources at the level of brain connectivity. OSCINE-NET.ORG fills this gap by offering detailed connectivity data in a user-friendly, interactive visual format.

The interactive nature of this resource offers many advantages over a static diagram or simple connectivity matrix. Users can display select networks, such as the rich broker club and vocal control network, facilitating exploration of their interactions with each other or the rest of the brain. Focused inspection of network components is easily accomplished by selecting any number of nodes or connections to view in isolation, as well as by using the focus button to move one synapse up or down. Further information is accessible in the side panel for each connection, including citations and information about the species, sex, and age of subjects used in the cited studies. Overall, this tool provides unprecedented ease of access to all known songbird connectivity data, offering many opportunities for deeper inquiry at multiple levels. We highlight a few specific use cases in the following sections.

## Community functions and circuitry

Communities are defined by their high internal connectivity. We find that larger functional circuits that have

been previously defined are often contained within each community. Although the motor community contains most of the motor production circuits, it also contains many visceral sensory feedback circuits, which highlights the essential role of sensory-motor circuitry integration for motor production. The visual community contains a variety of functional visual circuits essential to complex, visually-guided behaviors. For instance, it contains circuits for sensory processing of the visual environment, as well as centrifugal and motor control circuits integral to navigating the outside world during flight [45, 46]. The associative community contains NCL, the main associative learning region of the songbird brain which is often considered the center of cognitive control and executive function [47, 49, 69]. This community also contains major portions of thalamofugal and tectofugal visual pathways [70], trigeminal sensorimotor circuits for orofacial control [71], somatosensory integration circuits and the source of the pyramidal tract [50, 51, 72], as well as circuits essential to sexual imprinting [73]. In addition to the social behavior network, the social community contains septo-hippocampal circuits integral to learning and memory [55] and viscerolimbic circuitry that is essential to motivationally-driven behaviors and homeostatic responses [56]. The auditory community contains perceptual and associative circuits of the auditory pathway—including those involved in individual and species recognition [74–77], as well as those thought to be involved in sensorimotor integration of a bird's own vocal production [78]. As already described in detail, the vocal community contains the majority of the canonical vocal control network, as well as nodes implicated by other people as part of the circuits regulating vocal learning and production. Some of those non-canonical nodes and theorized circuits will be expanded upon in the following subsection. Thus, these communities contain a variety of functional circuitry, and their designations are a useful anchor for considering what connectivity across these communities might mean for complex behaviors.

We find that a subset of sub-communities connect with other communities significantly more than by chance,

(See figure on next page.)

**Fig. 5** A small number of nodes occupy a distinct connectivity space: the “rich broker club.” **A** Principal component analysis for dimensionality reduction and k-means clustering parses out one cluster (blue, “Cluster 2”) that is distinctly different from the others. **B** Comparison of the observed (black solid line) and random mean (blue dotted line) relationships between rich club coefficients and degree. The point at which an observed relationship exits the standard deviation (blue shading) of the random mean marks the degree threshold above which nodes in our network are connected more than what would be expected in a randomly connected network of the same size (48, arrowhead). **C** Nodes plotted by betweenness centrality and degree separate the same cluster of nodes revealed in **A**, which we deem the “rich broker club.” See additional files for a table of these and other values for each node (Additional file 3). **D** Anatomical connections between the members of the rich broker club. Nodes are colored based on community membership and organized by superstructure. In-degree (**E**) and out-degree (**F**) of each member of the rich broker club are represented as stacked bar plots grouped by community. Bars are organized with each node's highest community degree value closest to the x-axis, followed by the second-highest, and so on

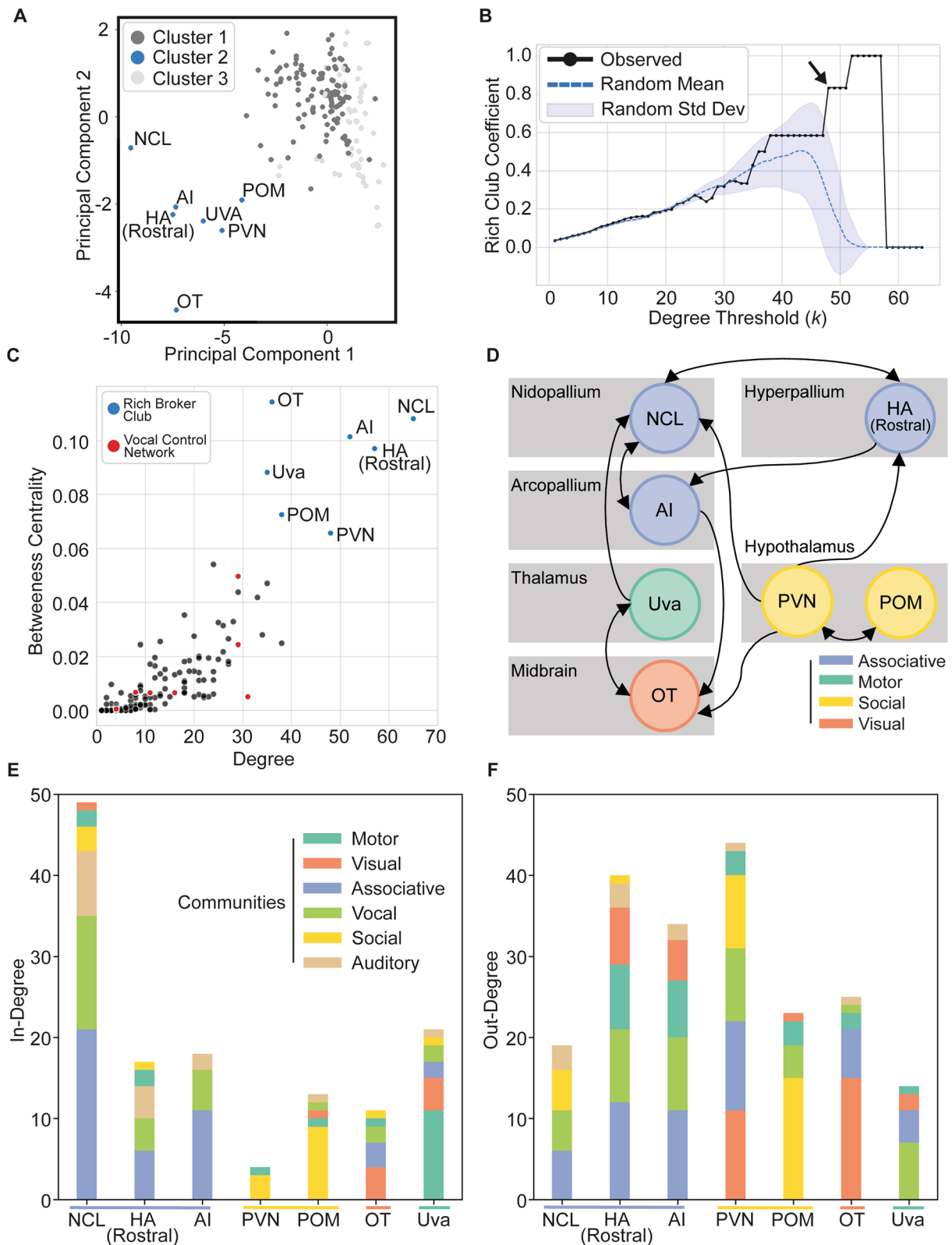


**Fig. 5** (See legend on previous page.)

**Table 4** Node-level connectivity metrics for nodes in the top 5% for at least one metric

Node	Degree	In-Degree	Out-Degree	Betweenness centrality
NCL	<b>65</b>	<b>49</b>	16	<b>0.108</b>
HA (Rostral)	<b>57</b>	<b>17</b>	<b>40</b>	<b>0.097</b>
AI	<b>52</b>	<b>18</b>	<b>34</b>	<b>0.101</b>
PVN	<b>48</b>	4	<b>44</b>	<b>0.066</b>
POM	<b>38</b>	13	<b>25</b>	<b>0.073</b>
AIV	<b>38</b>	10	<b>28</b>	0.025
OT	<b>36</b>	11	<b>25</b>	<b>0.114</b>
Uva	<b>35</b>	<b>21</b>	14	<b>0.088</b>
DLHp	<b>35</b>	11	<b>24</b>	0.047
NIL	34	<b>25</b>	9	0.028
HA (Caudal)	33	14	<b>19</b>	0.042
Area X	31	<b>29</b>	2	0.005
RA	29	14	15	<b>0.050</b>
HVC	29	<b>17</b>	12	0.024
VP	27	<b>17</b>	10	0.027
LoC	27	5	<b>22</b>	0.018
ICo	25	<b>19</b>	6	0.019
RAm	24	10	14	<b>0.054</b>
MSt	23	<b>19</b>	4	0.005
CSt	20	<b>17</b>	3	0.005

We present degree (also split into in- and out-degree) and betweenness centrality. Entries are presented in descending order of degree. Bolded entries represent those that are in the top 5% of the entire network

suggesting ethologically relevant aspects of songbird brain connectivity, particularly in vocal learning and production. The vocal community comprises two sub-communities (Table 3). The first, vocal sub-community 4a, preferentially receives inputs from auditory sub-community 6a, which contains circuits essential for higher-order auditory perception and individual recognition. This suggests potential underpinnings for how real-time auditory signal processing can directly impact vocalizations and timing, such as during courtship interactions or territorial displays [79, 80]. Vocal sub-community 4a also has reciprocal connections with both associative sub-communities (3a and 3b), which include circuits for higher-order visual perception, somatosensory integration, and fine motor control. This further emphasizes the potential for multisensory circuits to impact vocal circuits [19–22]. In addition, vocal sub-community 4b preferentially receives inputs from social sub-community 5a, which includes most nodes in the social behavior network. This anatomical connectivity supports a functional relationship between social and vocal learning circuits [57], including substrates by which the social behavior network may directly impact the vocal control network. Thus, combining community modularity and

sub-community preferential connectivity provides novel insight into how multiple information streams are integrated for meaningful behavioral output. It also helps identify which functional circuits might be of particular importance, offering a targeted approach for further study of nodes and circuits essential for complex behaviors.

Significant connectivity across sub-communities highlights anatomical bases of potential interest for future study. For instance, the caudolateral nidopallium (CLM), part of auditory sub-community 6a, projects to the nucleus interfacialis (Nif) in vocal sub-community 4a. CLM is integral to higher auditory processing circuits involved in individual and species recognition [61, 74]. Nif relays auditory information to other vocal community nodes, including HVC [81]. Connections between CLM and Nif are likely an integral part of the functional circuitry for auditory-vocal integration. Similarly, POM, a member of social sub-community 5a, connects to the ventral tegmental area (VTA) in vocal sub-community 4b. POM is thought to be a main driver of sexually-motivated singing [82–84]. VTA is involved in the reward aspects of vocalizations and delivers dopamine to the vocal control network in a social-context-dependent manner during singing [27]. Connections between POM and VTA therefore might be an essential part of functional circuits for social-vocal integration. Although individual connections for each of these complex behaviors are well-defined, the full scope of the functional circuits are not. Significant connectivity across sub-communities suggests many other such connections, including the few highlighted here, for further investigation. The data reported in this study, combined with the tool provided at OSCINE-NET.ORG, provide inroads for defining these functional circuits more completely.

#### Beyond the canonical vocal control network

The connectivity data presented at OSCINE-NET.ORG and the functional communities discussed in the present study provide a thorough anatomical basis that, combined with other functional knowledge of these nodes and circuits, offer complimentary evidence towards describing the neural underpinnings of vocal behavior. The vocal community includes five nodes of the canonical vocal control network. In addition, it contains several non-canonical nodes studied as part of a broader “song system,” as well as several other non-canonical nodes that have yet to be extensively studied for their relevance to vocal learning and production. We can better understand the contribution of these non-canonical nodes to functional circuitry for vocal control by considering both their inclusion in the vocal sub-communities and their significant inputs from auditory and social sub-communities.

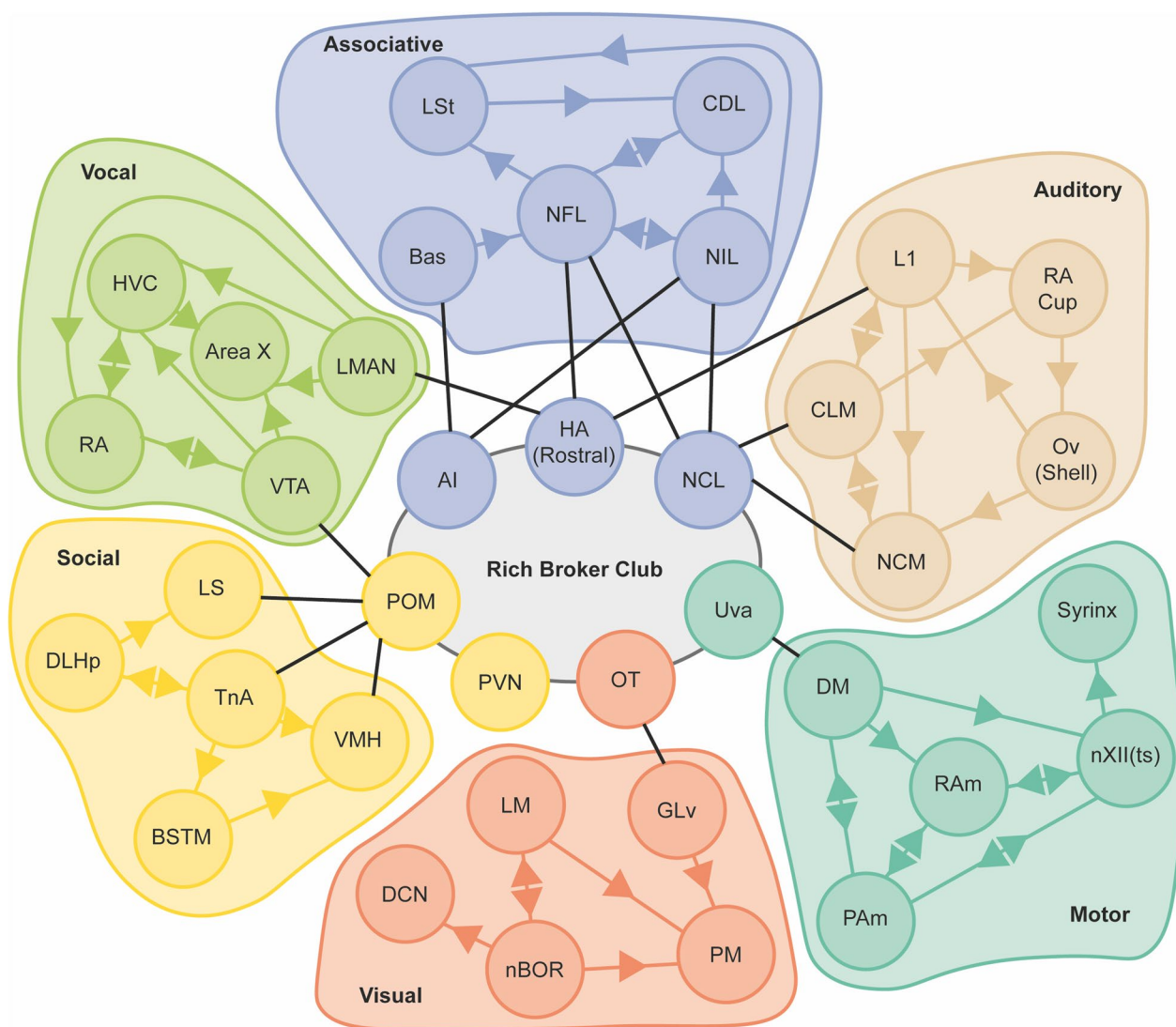


**Fig. 6** The rich broker club connects functional networks necessary for vocal learning. A visual representation of how the rich broker club could act as a collective liaison between functional communities. Represented nodes in each community were selected based on functional relevance for vocal learning and/or high degree. Within communities, all connectivity between selected nodes are shown. Between rich broker club members and selected nodes, only bidirectional connectivity (black lines) is shown. Directionality of all other connections is marked by arrowheads. All connectivity from rich broker nodes can be found at OSCINE-NET.ORG

This targeted approach will help identify which of these nodes should be included in an expanded concept of the vocal control network.

Nif and VTA are both members of the vocal community and have well-defined roles in vocal learning, showing intriguing connectivity with canonical vocal control network nodes and other nodes in the vocal community broadly. The fact that each of these nodes are within the vocal community indicates their high interconnectivity with other nodes in the vocal community, including the canonical vocal control network. Nif forms bidirectional connections with HVC, and directly influences the

timing of song elements during vocal learning [54]. VTA provides dopaminergic inputs to Area X, influencing song variability and learning through an intrinsic reward-prediction error signal [28, 53]. The ventral pallidum (VP) receives input from Area X and forms bidirectional connections with HVC, RA, DLM, and VTA, playing a significant role in performance evaluation during developmental vocal learning [52]. Other, less-studied nodes in the vocal community show compelling evidence of their importance for vocal learning. For instance, the lateral habenula (LHb) is activated by VP and inhibits dopamine neurons in VTA. Lesioning LHb in juveniles, but

not adults, results in abnormal song structure [85], implicating LHB in dopaminergic reward-related regulation of developmental vocal learning. Thus, our anatomical data and graph theoretical analyses complement other functional research. This allows functional and behavioral observations to be grounded in brain-wide connectivity data, further unifying research on non-canonical vocal control network nodes, and offering a strong foundation for considering an expanded concept of the vocal control network.

While our community analysis finds the majority of canonical vocal control network nodes to be part of the vocal community, there is an interesting separation of these nodes across the vocal sub-communities. Pallial RA clusters with thalamic DLM in vocal sub-community 4b, away from the other pallial vocal control network nodes (HVC and LMAN) in vocal sub-community 4a. Work supporting a motor theory of vocal evolution [86] posits that the vocal control network evolved out of a more ancient common motor production circuit, in particular that RA, a vocal-specialist node, evolved out of the surrounding motor-general arcopallium. This theory is supported by more recent work highlighting molecular specializations of RA compared to the surrounding arcopallium [87, 88], particularly in its projection neurons. Learned vocal behavior requires the coordination of multiple body systems (e.g., vocal musculature, respiratory systems, auditory feedback networks, etc.), and thus likely more distributed subpallial circuits than limb or body movements. Indeed, our data show RA is more connected with subpallial nodes (20 nodes) than with other nodes in the pallium (6 nodes). This profile is more similar to other nodes in vocal sub-community 4b, such as VP (connected to 17 subpallial & 4 pallial nodes) or LoC (connected to 15 subpallial & 10 pallial nodes), and more dissimilar from vocal sub-community 4a nodes like HVC (connected to 9 subpallial & 16 pallial nodes) or LMAN (connected to 5 subpallial & 9 pallial nodes). Since sub-communities are computationally defined by similar connectivity profiles, this clustering of RA with more subpallial-connected nodes, and away from more pallial-connected nodes, seems anatomically justified. Of note, RA is the only pallial node in vocal sub-community 4b, further supporting an argument that the specialization of RA for vocal learning might be more in its subpallial outputs than its pallial inputs.

#### **The rich broker club as a liaison, connecting all communities and multiple functional circuits**

The rich broker club is well-suited for orchestrating the global exchange of information across the brain, more so than any single community. These nodes exhibit some of the highest connectivity with the rest of the network,

indicating their capacity to share information widely. They act as brokers by directly connecting pairs of nodes in separate communities that may otherwise not be connected. For example, NCL (associative) is bidirectionally connected to both the dorsal arcopallium (AD, vocal) and CLM (auditory), which have no direct connections to each other. Due to their bidirectional connectivity with multiple communities, the rich broker club nodes facilitate communication between functional circuits. Collectively, this club accounts for ~30% of all network connections, directly links ~70% of all nodes, and bridges every community and superstructure in the brain. This club is thus in a strong position to act as a liaison, coordinating information transfer between nearly any two functional circuits, and potentially representing an important multisensory integration circuit directly impinging upon a number of complex learned behaviors.

The connections between the rich broker club and their respective communities provide valuable insight into global network architecture and channels for information flow. For example, although the vocal community lacks a node in the rich broker club, it receives inputs from every node of this club and sends outputs to six of the seven nodes. The vocal community has bidirectional connectivity with rich broker club members in the associative (NCL, AI, and HA [Rostral]) and social (POM) communities. This connectivity suggests that vocal behaviors may be influenced by higher-order associative and cognitive circuits. For instance, firing patterns of vocalization-correlated neurons in NCL increase immediately prior to voluntary vocalizations, implicating cognitive control of vocal behavior [48]. NCL is also intimately involved in cue-based counting, a type of motor-planning of vocalizations that is a hallmark of executive function [49]. In addition, HA (Rostral) is a major somatosensory hub in the songbird brain, and passes this body sensory information to Nif in the vocal community [89]. Given the central role of coordinating body and vocal-motor movements during courtship in many songbirds [90–92], it is possible that this and other bidirectional connections are essential components of that functional circuit. This context-dependency of vocal behavior undoubtedly relies on multiple integrated functional circuits. Further investigation of the rich broker club and its connectivity would help identify the integral communities, nodes, and connections involved in these complex functional circuits.

#### **Limitations**

Our data reflect the current state of reported literature and serve as a call to action for further research to better understand the biology underlying these complex brain networks. The field has primarily focused on adult male zebra finches—this lack of diversity in age, sex,

and species restricts our ability to appreciate and interrogate cross- and within-species differences, limiting the generalizability of our findings. These studies have also disproportionately focused on describing the anatomical connections of a few nodes, particularly in the vocal control network, leaving many gaps in our knowledge that merit further focused inquiry. In addition, representing the connectome as a single hemisphere excludes contralateral connectivity, preventing appreciation of the brain's bilateral nature, and of potential lateralization in circuitry underlying complex learned behaviors [93–95]. Similarly, there are many brain regions, like the oval nucleus of the mesopallium, defined on functional, neurochemical, gene expression, or other grounds that are not represented in our dataset due to a lack of anatomical connectivity data [23]. These nodes and their connections are undoubtedly important for defining network structure and interrogating the totality of circuitry contributing to complex learned behaviors, and must be further probed at an anatomical level. Finally, the size of our defined nodes might exert a particular influence on their connectivity metrics and overall network structure as described here. Of note, two members of the rich broker club (NCL and Uva) have vastly different volumes and cell densities. While outside the scope of this study, incorporating such volumetric or cell density weighting to nodes—as well as excitatory, inhibitory, or neuromodulatory nature to connections—would add additional levels of information essential for describing global network architecture. Future work must address these limitations to provide a more complete picture of the songbird brain's connectivity, and parse its implications for complex learned behaviors.

## Conclusion

By assessing connectivity in the songbird brain at global and local levels, we find support for efficiency and robustness (small-worldness), functional modularity (communities), and a small set of highly influential brain areas (rich broker club). The rich broker club is highly connected at multiple levels—to other nodes, communities, and superstructures, as well as between themselves—and connects about two-thirds of nodes in the brain, accounting for approximately one-third of known connections. OSCINE-NET.ORG is the first mesoscale connectome for any songbird, and the first open-source and public connectome for any vocal learner. It will serve as a powerful tool for the broader research community, enabling further exploration of brain-wide connectivity and its implications for complex learned behaviors.

## Abbreviations

A8 Dopaminergic Cell Group A8  
AA Anterior Arcopallium

AD Dorsal Arcopallium  
AH Anterior Hypothalamus  
AI Intermediate Arcopallium  
AIV Ventral Intermediate Arcopallium  
ALp Posterior Nucleus of the Ansa Lenticularis  
AM Medial Arcopallium  
Area X Used as a proper name  
Av Avalanche  
Bas Nucleus Basorostralis  
BSTL Lateral Bed Nucleus of the Stria Terminalis  
BSTM Medial Bed Nucleus of the Stria Terminalis  
CDL Dorsolateral Corticoid Area  
CG Central Gray  
CLM Caudolateral Mesopallium  
CMM Caudomedial Mesopallium  
CSt Caudal Striatum  
Cu Cuneate Nucleus  
CuE External Cuneate Nucleus  
D Nucleus of Darkschewitsch  
DCN Deep Cerebellar Nuclei  
DIP Dorsointermediate Thalamus, Posterior Nucleus  
DIVA Dorsointermediate Thalamus, Ventroanterior Nucleus  
DLA Dorsolateral Thalamus, Anterior Nucleus  
DLHp Dorsolateral subregion of Hippocampus  
DLL Dorsolateral Thalamus, Lateral Nucleus  
DLM Dorsolateral Thalamus, Medial Nucleus  
DLP Dorsolateral Thalamus, Posterior Nucleus  
DM Dorsomedial Nucleus of the Intercollicular Complex  
DMA Dorsomedial Thalamus, Anterior Nucleus  
DMHp Dorsomedial subregion of Hippocampus  
DMP Dorsomedial Thalamus, Posterior Nucleus  
DT (CbN) Cerebellar-recipient Dorsal Thalamus  
E Entopallium  
EM Ectomammillary Nucleus  
Ep Perientopallium  
FLM Frontal Lateral Mesopallium  
FRL Lateral part of the Mesencephalic Reticular Formation  
FRM Medial part of the Mesencephalic Reticular Formation  
G Gracile nucleus  
GLv Ventral portion of the Lateral Geniculate Nucleus  
GP Globus Pallidus  
HA (Caudal) Hyperpallium Apicale, Caudal Portion  
HA (Rostral) Hyperpallium Apicale, Rostral Portion  
HD Hyperpallium Densocellulare  
HI Intercalated part of the Hyperpallium  
HVC Used as a proper name  
HVC Shelf Shelf of HVC  
IC Interstitial Nucleus of Cajal  
ICo Intercollicular Nucleus  
IHA Interstitial part of the Hyperpallium Apicale  
ILM Intermediate Lateral Mesopallium  
Imc Nucleus Isthmi, pars magnocellularis  
IMM Intermediate Medial Mesopallium  
IO Inferior Olive  
ION Nucleus Isthmo-Opticus  
IOS Nucleus Infra-Olivarius Superior  
Ipc Nucleus Isthmi, pars parvocellularis  
IPS Nucleus Interstitio-Praetecto-Subpretectalis  
L1 Field L1  
L2a Field L2a  
L2b Field L2b  
L3 Field L3  
LHb Lateral Habenula  
LHY Lateral Hypothalamus  
LLD Dorsal Nucleus of the Lateral Lemniscus  
LLI Intermediate Nucleus of the Lateral Lemniscus  
LLV Ventral Nucleus of the Lateral Lemniscus  
LM Nucleus Lentiformis Mesencephali  
LMAN Lateral Magnocellular Nucleus of the Anterior Nidopallium  
LoC Locus Coeruleus  
LPC Nucleus Laminaris Precommissuralis

LS	Lateral Septum
LSt	Lateral Striatum
MD	Dorsal Mesopallium
MHb	Medial Habenula
MLd	Dorsal part of the Lateral Mesencephalic Nucleus
MMAN	Medial Magnocellular Nucleus of the Anterior Nidopallium
MS	Medial Septum
MSt	Medial Striatum
MV	Trigeminal Motor Nucleus
MVId	Dorsal Subnucleus of the Facial Motor Nucleus
MVIlv	Ventral Subnucleus of the Facial Motor Nucleus
MVL	Nucleus of the Ventrolateral Mesopallium
nA	Nucleus Ambiguus
NA	Nucleus Angularis
nAc	Nucleus Accumbens
nBOR	Nucleus of the Basal Optic Root
NCL	Caudolateral Nidopallium
NCM	Caudomedial Nidopallium
NDB	Nucleus of the Diagonal Band
NFL	Frontal Lateral Nidopallium
NFM	Frontal Medial Nidopallium
nHpC	Nucleus of the Hippocampal Commissure
NIf	Nucleus Interfacialis
nIII	Nucleus of the Third Cranial Nerve
NIL	Lateral Intermediate Nidopallium
NIM	Medial Intermediate Nidopallium
nIV	Nucleus of the Fourth Cranial Nerve
nIXr	Glossopharyngeal Motor Nucleus, retrofacial portion
NL	Nucleus Laminaris
NM	Nucleus Magnocellularis
NR	Red Nucleus
nTOv	Nucleus of the Tractus Ovoidalis
nTS	Nucleus of the Solitary Tract
nTTDc	Nuclei of the Descending Trigeminal Tract, pars caudalis
nTTDi	Nuclei of the Descending Trigeminal Tract, pars interparalis
nTTDo	Nuclei of the Descending Trigeminal Tract, pars oralis
nX	Motor Nucleus of the Vagus
nXII(I)	Hypoglossal Nucleus of the Twelfth Cranial Nerve, Lingual Portion
nXII(ts)	Hypoglossal Nucleus of the Twelfth Cranial Nerve, Tracheosyringeal Portion
OCb	Oculomotor cerebellum
OT	Optic tectum
OTu	Olfactory Tubercle
Ov (Core)	Core of Nucleus Ovoidalis
Ov (Shell)	Shell of Nucleus Ovoidalis
PAm	Nucleus Paraambiguus
paraHVC	Used as a proper name
PBvl	Ventrolateral Portion of the Parabrachial Nucleus
PL	Lateral Pontine Nucleus
PLL	Paralateral Lemniscal Nucleus
PM	Medial Pontine Nucleus
POA	Preoptic Area of the Hypothalamus (excluding the medial nucleus)
PoA	Posterior Nucleus of the Pallial Amygdala
POM	Medial Preoptic Nucleus of the Hypothalamus
PPC	Nucleus Principalis Precommissuralis
PPT	Pedunculopontine Tegmental Nucleus
PrV	Principal Sensory Trigeminal Nucleus
PT	Nucleus Pretectalis
PVN	Paraventricular Nucleus of the Hypothalamus
R	Nucleus Raphe
RA	Robust Nucleus of the Arcopallium
RA Cup	Cup of the Robust Nucleus of the Arcopallium
RAm	Nucleus Retroambiguus
Retina DGCS	Displaced Ganglion Cells
Retina RGCs	Retinal Ganglion Cells
RPcdl	Parvocellular Reticular Formation of the caudal pons, dorsolateral portion
RPcvm	Parvocellular Reticular Formation of the caudal pons, ventromedial portion

RPgc	Reticular Nucleus of the Caudal Pons, Gigantocellular Part
RS	Nucleus Reticularis Superior of the Thalamus (dorsal and ventral portions)
Rt	Nucleus Rotundus
RVL	Rostral Ventrolateral Medulla
SC	Subcoeruleus
SCE	External Cellular Stratum of the Lateral Hypothalamus
SCN	Suprachiasmatic Nuclei
SHb	Subhabenular Nucleus
Slu	Nucleus Semilunaris
SN	Substantia Nigra (pars compacta and pars reticulata)
SO	Superior Olive
SON	Supraoptic Nuclei
sP	Nucleus Subprincipalis
SpA	Subpallial Amygdaloid Area
SPC	Parvocellular Part of the Superficial Nucleus of the Thalamus
SpL	Nucleus Spiriformis Lateralis
SpM	Nucleus Spiriformis Medialis
SPT	Nucleus Subpretectalis
SRT	Nucleus Subrotundus
STN	Subthalamic Nucleus
TnA	Nucleus Taeniae of the Amygdala
Tu	Tuberal Nucleus of the Hypothalamus
Uva	Nucleus Uvaeformis
VbC	Vestibular Cerebellum
VeD	Descending Vestibular Nucleus
VeL	Lateral Vestibular Nucleus
VeM	Medial Vestibular Nucleus
VeS	Superior Vestibular Nucleus
VHp	Ventral subregion of Hippocampus
VMH	Ventromedial Nucleus of the Hypothalamus
VP	Ventral Pallidum
VTA	Ventral Tegmental Area

## Supplementary Information

The online version contains supplementary material available at <https://doi.org/10.1186/s12868-024-00919-3>.

**Additional file 1.** All raw data from OSCINE-NET.ORG. An excel workbook containing all the nodes, connections, and metadata descriptions contained in the OSCINE-NET.ORG database as of July 26, 2024. This is the complete dataset that was used for graph theoretical analysis in Savoy, Anderson & Gogola 2024.

**Additional file 2.** Citations supporting connectivity data presented at OSCINE-NET.ORG. A table of all citations included in database and map presented in Savoy, Anderson & Gogola 2024, including the number of connections each citation supports.

**Additional file 3.** All nodes and their associated node-level metrics. A table of all node-level metrics presented in Savoy, Anderson & Gogola 2024. These metrics include degree centrality, betweenness centrality, degree, in-degree, out-degree, closeness centrality, and clustering coefficient.

## Acknowledgements

We acknowledge Drs. Daniel Margoliash, Osceola Whitney, and Bobby Kasthuri for their unwavering support. We thank Dr. Murray Shanahan for sharing data and code from Shanahan et al. (2013) and Logan Thomas for his contributions to the initial map design. We acknowledge Dr. Kevin Boergens, Henry Jones, and Dr. Anshuman Swain for initial graph theory assistance and helpful discussions.

## Author contributions

The authors confirm their contributions to the paper as follows. Original conception: AS. Project design: all authors. Data collection and error checking: all authors. Graph theoretical analyses: AS. Interpretation: all authors. Figure preparation: all authors. Writing: all authors. Oversight: JVG. All authors reviewed the results and approved the final version of the manuscript.

**Funding**

No grant funding contributed to this project.

**Availability of data and materials**

Code and datasets for this study are available in a Google Drive account associated with the correspondence address: <https://drive.google.com/drive/folders/1eFj8hN9Ze0Rsk6fOnE-hl4CC4BZBxjn>.

**Declarations****Ethics approval and consent to participate**

Not applicable.

**Consent for publication**

Not applicable.

**Competing interests**

The authors declare no competing interests.

**Author details**

<sup>1</sup>Department of Psychology, Integrative Neuroscience Program, University of Chicago, 5848 S University Ave, Chicago, IL 60637, USA. <sup>2</sup>Department of Molecular, Cellular, and Developmental Biology, The City University of New York Graduate Center, 365 5th Ave, New York, NY 10016, USA. <sup>3</sup>Department of Biology, The City College of the City University of New York, 160 Convent Ave, New York, NY 10031, USA. <sup>4</sup>Department of Medicine, The University of Chicago, 5841 S Maryland Ave, Chicago, IL 60637, USA.

Received: 26 July 2024 Accepted: 12 December 2024

Published online: 27 December 2024

**References**

- Knudsen EI. Auditory and visual maps of space in the optic tectum of the owl. *J Neurosci Off J Soc Neurosci*. 1982;2(9):1177–94.
- Bergan JF, Knudsen EI. Visual modulation of auditory responses in the owl inferior colliculus. *J Neurophysiol*. 2009;101(6):2924–33.
- Knudsen EI. Early auditory experience aligns the auditory map of space in the optic tectum of the barn owl. *Science*. 1983;222(4626):939–42.
- Lim MM, Murphy AZ, Young LJ. Ventral striatopallidal oxytocin and vasopressin V1a receptors in the monogamous prairie vole (*Microtus ochrogaster*). *J Comp Neurol*. 2004;468(4):555–70.
- Pitkow LJ, Sharer CA, Ren X, Insel TR, Terwilliger EF, Young LJ. Facilitation of affiliation and pair-bond formation by vasopressin receptor gene transfer into the ventral forebrain of a monogamous vole. *J Neurosci Off J Soc Neurosci*. 2001;21(18):7392–6.
- Bergson C, Mrzljak L, Smiley JF, Pappy M, Levenson R, Goldman-Rakic PS. Regional, cellular, and subcellular variations in the distribution of D1 and D5 dopamine receptors in primate brain. *J Neurosci Off J Soc Neurosci*. 1995;15(12):7821–36.
- Mars RB, Jbabdi S, Sallet J, O'Reilly JX, Croxson PL, Olivier E, et al. Diffusion-weighted imaging tractography-based parcellation of the human parietal cortex and comparison with human and macaque resting-state functional connectivity. *J Neurosci Off J Soc Neurosci*. 2011;31(11):4087–100.
- Dorkenwald S, Matsliah A, Sterling AR, Schlegel P, Yu S chieh, McKellar CE, et al. Neuronal wiring diagram of an adult brain. *bioRxiv*; 2023, <https://doi.org/10.1101/2023.06.27.546656v2>
- Schlegel P, Yin Y, Bates AS, Dorkenwald S, Eichler K, Brooks P, et al. Whole-brain annotation and multi-connectome cell typing quantifies circuit stereotypy in *Drosophila*. *BioRxiv Prepr Serv Biol*. 2023;2023.06.27.546055.
- Zheng Z, Lauritzen JS, Perlman E, Robinson CG, Nichols M, Milkie D, et al. A complete electron microscopy volume of the brain of adult *Drosophila melanogaster*. *Cell*. 2018;174(3):730–743.e22.
- Buhmann J, Sheridan A, Malin-Mayor C, Schlegel P, Gerhard S, Kazimiers T, et al. Automatic detection of synaptic partners in a whole-brain *Drosophila* electron microscopy data set. *Nat Methods*. 2021;18(7):771–4.
- Heinrich L, Funke J, Pape C, Nunez-Iglesias J, Saalfeld S. Synaptic cleft segmentation in non-isotropic volume electron microscopy of the complete *Drosophila* brain. In: Frangi AF, Schnabel JA, Davatzikos C, Alberola-López C, Fichtinger G, editors. *Medical Image Computing and Computer Assisted Intervention – MICCAI 2018*. Cham: Springer International Publishing; 2018. p. 317–25.
- Majka P, Bai S, Bakola S, Bednarek S, Chan JM, Jermakow N, et al. Open access resource for cellular-resolution analyses of corticocortical connectivity in the marmoset monkey. *Nat Commun*. 2020;11(1):1133.
- Oh SW, Harris JA, Ng L, Winslow B, Cain N, Mihalas S, et al. A mesoscale connectome of the mouse brain. *Nature*. 2014;508(7495):207–14.
- Chon U, Vanselow DJ, Cheng KC, Kim Y. Enhanced and unified anatomical labeling for a common mouse brain atlas. *Nat Commun*. 2019;10(1):5067.
- Vates GE, Nottebohm F. Feedback circuitry within a song-learning pathway. *Proc Natl Acad Sci*. 1995;92(11):5139–43.
- Vates GE, Vicario DS, Nottebohm F. Reafferent thalamo-cortical loops in the song system of oscine songbirds. *J Comp Neurol*. 1997;380(2):275–90.
- Nottebohm F, Stokes TM, Leonard CM. Central control of song in the canary. *Serinus canarius J Comp Neurol*. 1976;165(4):457–86.
- Kimball MG, Gautreaux EB, Couvillion KE, Kelly TR, Stansberry KR, Lattin CR. Novel objects alter immediate early gene expression globally for ZENK and regionally for c-Fos in neophobic and non-neophobic house sparrows. *Behav Brain Res*. 2022;25(428): 113863.
- Kruse AA, Stripling R, Clayton DF. Context-specific habituation of the *zenk* gene response to song in adult zebra finches. *Neurobiol Learn Mem*. 2004;82(2):99–108.
- Tokarev K, Tiunova A, Scharff C, Anokhin K. Food for song: expression of c-fos and ZENK in the zebra finch song nuclei during food aversion learning. *PLoS ONE*. 2011;6(6): e21157.
- Menardy F, Giret N, Del Negro C. The presence of an audience modulates responses to familiar call stimuli in the male zebra finch forebrain. *Eur J Neurosci*. 2014;40(9):3338–50.
- Jarvis ED, Scharff C, Grossman MR, Ramos JA, Nottebohm F. For whom the bird sings: context-dependent gene expression. *Neuron*. 1998;21(4):775–88.
- Chen Y, Matheson LE, Sakata JT. Mechanisms underlying the social enhancement of vocal learning in songbirds. *Proc Natl Acad Sci U S A*. 2016;113(24):6641–6.
- Carouso-Peck S, Goldstein MH. Female social feedback reveals non-imitative mechanisms of vocal learning in zebra finches. *Curr Biol*. 2019;29(4):631–636.e3.
- Wall EM, Woolley SC. Social experiences shape song preference learning independently of developmental exposure to song. *Proc Biol Sci*. 2024;291(2024):20240358.
- Roeser A, Gadagkar V, Das A, Puzerey PA, Kardon B, Goldberg JH. Dopaminergic error signals retune to social feedback during courtship. *Nature*. 2023;623(7986):375–80.
- Gadagkar V, Puzerey PA, Chen R, Baird-Daniel E, Farhang AR, Goldberg JH. Dopamine neurons encode performance error in singing birds. *Science*. 2016;354(6317):1278–82.
- Louder MIM, Kuroda M, Taniguchi D, Komorowska-Müller JA, Morohashi Y, Takahashi M, et al. Transient sensorimotor projections in the developmental song learning period. *Cell Rep*. 2024;43(5): 114196.
- Reiner A, Perkel DJ, Bruce LL, Butler AB, Csillag A, Kuenzel W, et al. Revised nomenclature for avian telencephalon and some related brainstem nuclei. *J Comp Neurol*. 2004;473(3):377–414.
- Mohr J, Mohr R. Kumu Inc. 2011. <http://kumu.io>. Accessed 26 July 2024.
- Hagberg A, Swart PJ, Schult DA. Exploring network structure, dynamics, and function using NetworkX. In *Los Alamos National Laboratory (LANL)*, Los Alamos, NM, USA; 2008. p. 11–6. <https://www.osti.gov/biblio/960616>
- Watts DJ, Strogatz SH. Collective dynamics of “small-world” networks. *Nature*. 1998;393(6684):440–2.
- Newman ME, Strogatz SH, Watts DJ. Random graphs with arbitrary degree distributions and their applications. *Phys Rev E Stat Nonlin Soft Matter Phys*. 2001;64(2 Pt 2): 026118.
- Newman MEJ. Assortative mixing in networks. *Phys Rev Lett*. 2002;89(20): 208701.
- Traag VA, Waltman L, van Eck NJ. From Louvain to Leiden: guaranteeing well-connected communities. *Sci Rep*. 2019;9(1):5233.
- Vinh NX, Epps J, Bailey J. Information theoretic measures for clusterings comparison: variants, properties, normalization and correction for chance. *JMLR*. 2010;11:2837–54.
- Rubinov M, Sporns O. Complex network measures of brain connectivity: uses and interpretations. *Neuroimage*. 2010;52(3):1059–69.

39. Colizza V, Flammini A, Serrano MA, Vespignani A. Detecting rich-club ordering in complex networks. *Nat Phys*. 2006;2(2):110–5.
40. Sporns O, Zwi JD. The small world of the cerebral cortex. *Neuroinformatics*. 2004;2(2):145–62.
41. Shanahan M, Bingman VP, Shimizu T, Wild M, Güntürkün O. Large-scale network organization in the avian forebrain: a connectivity matrix and theoretical analysis. *Front Comput Neurosci*. 2013;7:89.
42. de Rus MA, van den Heuvel MP. Rich club organization and intermodule communication in the cat connectome. *J Neurosci Off J Soc Neurosci*. 2013;33(32):12929–39.
43. Harriger L, van den Heuvel MP, Sporns O. Rich club organization of macaque cerebral cortex and its role in network communication. *PLoS ONE*. 2012;7(9):e46497.
44. Gaede AH, Gutiérrez-Ibáñez C, Armstrong MS, Altshuler DL, Wylie DR. Pretectal projections to the oculomotor cerebellum in hummingbirds (*Calypte anna*), zebra finches (*Taeniopygia guttata*), and pigeons (*Columba livia*). *J Comp Neurol*. 2019;527(16):26442658.
45. Gaede AH, Gutiérrez-Ibáñez C, Wu PH, Pilon MC, Altshuler DL, Wylie DR. Topography of visual and somatosensory inputs to the pontine nuclei in zebra finches (*Taeniopygia guttata*). *J Comp Neurol*. 2024;532(2):e25556.
46. Wylie DR, Gaede AH, Gutiérrez-Ibáñez C, Wu P, Pilon MC, Azarogoo S, et al. Topography of optic flow processing in olivocerebellar pathways in zebra finches (*Taeniopygia guttata*). *J Comp Neurol*. 2023;531(6):640662.
47. Moll FW, Nieder A. Cross-modal associative mnemonic signals in crow endbrain neurons. *Curr Biol CB*. 2015;25(16):2196–201.
48. Brecht KF, Westendorff S, Nieder A. Neural correlates of cognitively controlled vocalizations in a corvid songbird. *Cell Rep*. 2023;42(3):112113.
49. Liao DA, Brecht KF, Veit L, Nieder A. Crows, “count” the number of self-generated vocalizations. *Science*. 2024;384(6698):874–7.
50. Wild JM, Williams MN. Rostral wulst of passerine birds: II. Intratelencephalic projections to nuclei associated with the auditory and song systems. *J Comp Neurol*. 1999;413(4):520–34.
51. Wild JM, Williams MN. Rostral Wulst in passerine birds: I. Origin, course, and terminations of an avian pyramidal tract. *J Comp Neurol*. 2000;416(4):429–50.
52. Chen R, Puzerey PA, Roeser AC, Riccelli TE, Podury A, Maher K, et al. Songbird ventral pallidum sends diverse performance error signals to dopaminergic midbrain. *Neuron*. 2019;103(2):266–276.e4.
53. Chen R, Gadagkar V, Roeser AC, Puzerey PA, Goldberg JH. Movement signaling in ventral pallidum and dopaminergic midbrain is gated by behavioral state in singing birds. *J Neurophysiol*. 2021;125(6):2219–27.
54. Zhao W, Garcia-Oscos F, Dinh D, Roberts TF. Inception of memories that guide vocal learning in the songbird. *Science*. 2019;366(6461):83–9.
55. Herold C, Schlömer P, Mafoppa-Fomat I, Mehlhorn J, Amunts K, Axer M. The hippocampus of birds in a view of evolutionary connectomics. *Cortex J Devoted Study Nerv Syst Behav*. 2019;118:165–87.
56. Kuenzel WJ, Medina L, Csillag A, Perkel DJ, Reiner A. The avian subpallium: new insights into structural and functional subdivisions occupying the lateral subpallial wall and their embryological origins. *Brain Res*. 2011;18(1424):67–101.
57. Anderson KL, Colón L, Doolittle V, Rosario Martinez R, Uruga J, Whitney O. Context-dependent activation of a social behavior brain network during learned vocal production. *Brain Struct Funct*. 2023;228(7):1785–97.
58. Krützfeldt NOE, Logerot P, Kubke MF, Wild JM. Connections of the auditory brainstem in a songbird, *Taeniopygia guttata*. I. Projections of nucleus angularis and nucleus laminaris to the auditory torus. *J Comp Neurol*. 2010;518(11):2109–34.
59. Krützfeldt NOE, Logerot P, Kubke MF, Wild JM. Connections of the auditory brainstem in a songbird, *Taeniopygia guttata*. II. Projections of nucleus angularis and nucleus laminaris to the superior olive and lateral lemniscal nuclei. *J Comp Neurol*. 2010;518(11):2135–48.
60. Wild JM, Krützfeldt NOE, Kubke MF. Connections of the auditory brainstem in a songbird, *Taeniopygia guttata*. III. Projections of the superior olive and lateral lemniscal nuclei. *J Comp Neurol*. 2010;518(11):2149–67.
61. Gobes SMH, Bolhuis JJ. Birdsong memory: a neural dissociation between song recognition and production. *Curr Biol CB*. 2007;17(9):789–93.
62. Knudsen DP, Gentner TQ. Mechanisms of song perception in oscine birds. *Brain Lang*. 2010;115(1):59–68.
63. Gentner TQ, Margoliash D. Neuronal populations and single cells representing learned auditory objects. *Nature*. 2003;424(6949):669–74.
64. Karten HJ, Brzozowska-Prechtl A, Lovell PV, Tang DD, Mello CV, Wang H, et al. Digital atlas of the zebra finch (*Taeniopygia guttata*) brain: a high resolution photo atlas. *J Comp Neurol*. 2013;521(16):3702–15.
65. Lovell PV, Wirthlin M, Kaser T, Buckner AA, Carleton JB, Snider BR, et al. ZEBRA: Zebra finch Expression Brain Atlas—a resource for comparative molecular neuroanatomy and brain evolution studies. *J Comp Neurol*. 2020;528(12):2099–131.
66. Nixdorf-Bergweiler BE, Bischof HJ. A stereotaxic atlas of the brain of the zebra finch, *Taeniopygia Guttata*: with special emphasis on telencephalic visual and song system nuclei in transverse and sagittal sections. Bethesda, MD: National Center for Biotechnology Information; 2007. <https://www.ncbi.nlm.nih.gov/books/NBK2355/>
67. De Groof G, George I, Touj S, Stacho M, Jonckers E, Cousillas H, et al. A three-dimensional digital atlas of the starling brain. *Brain Struct Funct*. 2016;221(4):1899–909.
68. Stokes TM, Leonard CM, Nottebohm F. The telencephalon, diencephalon, and mesencephalon of the canary, *Serinus canaria*, in stereotaxic coordinates. *J Comp Neurol*. 1974;156(3):337–74.
69. Kirschhock ME, Nieder A. Association neurons in the crow telencephalon link visual signs to numerical values. *Proc Natl Acad Sci U S A*. 2023;120(45):e2313923120.
70. Wild JM, Gaede AH. Second tectofugal pathway in a songbird (*Taeniopygia guttata*) revisited: tectal and lateral pontine projections to the posterior thalamus, thence to the intermediate nidopallium. *J Comp Neurol*. 2015;524(5):963–85.
71. Wild JM, Zeigler HP. Central projections and somatotopic organization of trigeminal primary afferents in pigeon (*Columba livia*). *J Comp Neurol*. 1996;368(1):136–52.
72. Wild JM, Williams MN. A direct cerebrocerebellar projection in adult birds and rats. *Neuroscience*. 2000;96(2):333–9.
73. Sadananda M, Bischof HJ. Afferentation of the lateral nidopallium: a tracing study of a brain area involved in sexual imprinting in the zebra finch (*Taeniopygia guttata*). *Brain Res*. 2006;1106(1):11–22.
74. Yu K, Wood WE, Johnston LG, Theunissen FE. Lesions to caudomedial nidopallium impair individual vocal recognition in the zebra finch. *J Neurosci*. 2023;43(14):2579–96.
75. Kudo T, Morohashi Y, Yazaki-Sugiyama Y. Early auditory experience modifies neuronal firing properties in the zebra finch auditory cortex. *Front Neural Circuits*. 2020;8(14):570174.
76. Bailey DJ, Wade J. Differential expression of the immediate early genes FOS and ZENK following auditory stimulation in the juvenile male and female zebra finch. *Mol Brain Res*. 2003;116(1):147–54.
77. Mello CV, Vates E, Okuhata S, Nottebohm F. Descending auditory pathways in the adult male zebra finch (*Taeniopygia Guttata*). *J Comp Neurol*. 1998;395(2):137–60.
78. Yip ZC, MillerSims VC, Bottjer SW. Morphology of axonal projections from the high vocal center to vocal motor cortex in songbirds. *J Comp Neurol*. 2012;520(12):27422756.
79. Jablonszky M, Zsebők S, Laczi M, Nagy G, Vaskuti É, Garamszegi LZ. The effect of social environment on bird song: listener-specific expression of a sexual signal. *Behav Ecol*. 2021;32(3):395–406.
80. Geberzahn N, Aubin T. How a songbird with a continuous singing style modulates its song when territorially challenged. *Behav Ecol Sociobiol*. 2014;68(1):1–12.
81. Coleman MJ, Mooney R. Synaptic transformations underlying highly selective auditory representations of learned birdsong. *J Neurosci Off J Soc Neurosci*. 2004;24(33):7251–65.
82. Riters LV, Ball GF. Lesions to the medial preoptic area affect singing in the male European starling (*Sturnus vulgaris*). *Horm Behav*. 1999;36(3):276–86.
83. Riters LV, Eens M, Pinxten R, Duffy DL, Balthazart J, Ball GF. Seasonal changes in courtship song and the medial preoptic area in male European starlings (*Sturnus vulgaris*). *Horm Behav*. 2000;38(4):250–61.
84. Saldanha CJ, Tuerk MJ, Kim YH, Fernandes AO, Arnold AP, Schlinger BA. Distribution and regulation of telencephalic aromatase expression in the zebra finch revealed with a specific antibody. *J Comp Neurol*. 2000;423(4):619–30.
85. Roeser A, Teoh HK, Chen R, Cohen I, Goldberg J. The songbird lateral habenula projects to dopaminergic midbrain and is important for normal vocal development. *Elife*. 2023. <https://doi.org/10.7554/eLife.90392.1>.

86. Feenders G, Liedvogel M, Rivas M, Zapka M, Horita H, Hara E, et al. Molecular mapping of movement-associated areas in the avian brain: a motor theory for vocal learning origin. *PLoS ONE*. 2008;3(3): e1768.
87. Mello CV, Kaser T, Buckner AA, Wirthlin M, Lovell PV. Molecular architecture of the zebra finch arcopallium. *J Comp Neurol*. 2019;527(15):2512–56.
88. Nevue AA, Zemel BM, Friedrich SR, Gersdorff H von, Mello CV. Cell type specializations of the vocal-motor cortex in songbirds. *Cell Rep*. 2023;42(11).
89. Wild JM. Visual and somatosensory inputs to the avian song system via nucleus uvaeformis (Uva) and a comparison with the projections of a similar thalamic nucleus in a nonsongbird, *columbia livia*. *J Comp Neurol*. 1994;349(4):512–35.
90. Ullrich R, Norton P, Scharff C, Waltzing *Taeniopygia*: integration of courtship song and dance in the domesticated Australian zebra finch. *Anim Behav*. 2016;1(112):285–300.
91. Ota N, Gahr M, Soma M. Tap dancing birds: the multimodal mutual courtship display of males and females in a socially monogamous songbird. *Sci Rep*. 2015;19(5):16614.
92. Cooper BG, Goller F. Partial muting leads to age-dependent modification of motor patterns underlying crystallized zebra finch song. *J Neurobiol*. 2004;61(3):317–32.
93. Rogers LJ, Koboroff A, Kaplan G. Lateral asymmetry of brain and behaviour in the zebra finch, *Taeniopygia guttata*. *Symmetry*. 2018;10(12):679.
94. Frank SY, Hunt JL, Bae AJ, Chirathivat N, Lotfi S, Raja SC, et al. Hemispheric dominance in HVC is experience-dependent in juvenile male zebra finches. *Sci Rep*. 2024;14(1):5781.
95. Floody OR, Arnold AP. Song lateralization in the zebra finch. *Horm Behav*. 1997;31(1):25–34.

### Publisher's Note

Springer Nature remains neutral with regard to jurisdictional claims in published maps and institutional affiliations.